Research Square

Preprints are preliminary reports that have not undergone peer review.
They should not be considered conclusive, used to inform clinical practice,
or referenced by the media as validated information.

Cross-host probiotic potential of an Exiguobacterium strain isolated from both sea cucumber (Apostichopus japonicus) and Manila clam (Ruditapes philippinarum)

Yaodong Qiu
Dalian Ocean University
Xinyan Zhao
Dalian Ocean University
Hui Guan
Dalian Ocean University
Xinghong Luo
Guangxi University
Liuqing Wang
Dalian Ocean University
Sitong Quan
Dalian Ocean University
Lei Fang
fanglei2014@dlou.edu.cn
Dalian Ocean University
Zhongming Huo
Dalian Ocean University

Research Article

Keywords: Exiguobacterium, Intestinal bacterium, Cross-host probiotic, Apostichopus japonicus, Ruditapes philippinarum, Whole genome sequencing

Posted Date: November 13th, 2026

DOI: https://doi.org/10.21203/rs.3.rs-11508627/v1

License: This work is licensed under a Creative Commons Attribution 4.0 International License.
Read Full License

Additional Declarations: No competing interests reported.

Cross-host probiotic potential of an *Exiguobacterium* strain isolated from both sea cucumber (*Apostichopus japonicus*) and Manila clam (*Ruditapes philippinarum*)

Yaodong Qiu[1,2] Xinyan Zhao[1,2] Hui Guan[2,3] Xinghong Luo[2,4] Liuqing Wang[2,3] Sitong Quan[1,2] Lei Fang[1,3,i] Zhongming Huo[2,3,ii]

1 College of Marine Science and Environment, Dalian Ocean University, Dalian 116023, China

2 Engineering Research Center of Shellfish Culture and Breeding, Dalian Ocean University, Dalian 116023, China

3 College of Fisheries and Life Science, Dalian Ocean University, Dalian 116023, China

4 College of Animal Science and Technology, Guangxi University, Nanning 530004, China

[i] Correspond to fanglei2014@dlou.edu.cn

[ii] Correspond to huozm@dlou.edu.cn

Abstract

Probiotics are being explored as sustainable alternatives to antibiotics in mariculture. However, host-derived strains with beneficial effects across multiple cultured species remain poorly characterized. In this study, an intestinal bacterium, strain AC31, was initially isolated from the intestinal tract of the sea cucumber *Apostichopus japonicus*, and its growth-promoting potential was confirmed in this host. Subsequently, a highly similar isolate, strain R27, was recovered from the intestines of the Manila clam *Ruditapes philippinarum*. Comparative molecular and whole-genome analyses demonstrated that the two isolates represented the same strain of *Exiguobacterium*, which was therefore designated AC31. Phenotypic characterization showed that strain AC31 was non-hemolytic, produced extracellular protease, amylase and lipase, and exhibited antioxidant activity and cell-surface properties suggestive of host adhesion. In host validation experiments, strain AC31 caused no obvious acute mortality in immersion assays and no apparent chronic toxicity during a 60-day culture trial. Dietary supplementation with strain AC31 improved growth-related indices in both *A. japonicus* and *R. philippinarum* and enabled colonization of the intestinal tracts of both hosts. Whole genome analysis further revealed genes involved in carbohydrate, protein and lipid metabolism, redox homeostasis and environmental adaptation, providing a genomic basis for its probiotic potential. No virulence factor genes were detected in the genome. Collectively, these findings imply that strain AC31 might be a promising cross-host probiotic candidate for sustainable mariculture.

Keywords

Exiguobacterium, Intestinal bacterium, Cross-host probiotic, *Apostichopus japonicus*, *Ruditapes philippinarum*, Whole genome sequencing

Introduction

Mariculture is a vital global industry that provides food nutrients, livelihood support, and ecological welfare for billions of people worldwide [1]. According to the State of World Fisheries and Aquaculture 2024 released by the Food and Agriculture Organization (FAO) of the United Nations, global aquatic animal production has grown steadily over the past seven decades, rising from 19 million tonnes in 1950 to 185 million tonnes in 2022 [2]. As a source of high-quality protein for the global population, aquatic animal farming also sustains employment opportunities and promotes regional economic development [3]. China has a long-standing mariculture industry and favorable geographical conditions, with its extensive coastline providing suitable environments for marine aquaculture development [4]. Currently, China is the world's largest mariculture producer, contributing 36% of global aquatic animal output in 2022, and plays a decisive role in safeguarding global food security and driving the sustainable development of the marine economy [5, 6]. Sea cucumber (*Apostichopus japonicus*) and Manila clam (*Ruditapes philippinarum*) are two representative and economically important marine aquaculture species in China. *A. japonicus*, a member of the family Stichopodidae, is valued for its nutritional value and medicinal properties [7, 8]. *R. philippinarum* is characterized by fast growth, high yield and wide consumer acceptance, occupying a dominant position in China's shellfish aquaculture industry [9]. According to the 2025 China Fisheries Statistical Yearbook, the national production of clams reached 4.74 million tonnes and sea cucumber production hit 326 thousand tonnes in 2024, jointly forming an important component of China's mariculture industry.

With the rapid expansion and intensification of mariculture, high-density farming has led to industrial bottlenecks, including deteriorating aquaculture water environments, reduced host immune competence, and frequent outbreaks of pathogenic diseases [10, 11]. These problems have caused substantial economic losses and restricted the sustainable development of modern mariculture [12]. Traditionally, antibiotics and chemical disinfectants have been widely applied to control pathogen proliferation and reduce disease incidence. However, long-term and excessive use of these agents has induced ecological and food safety risks, such as marine microbial community imbalance, antibiotic-resistant bacteria enrichment, and residual contamination of aquatic products [13].

Probiotics have emerged as safe, eco-friendly and sustainable alternatives to chemical antibiotics, becoming a research focus for green aquaculture technology [14]. Probiotics are defined as viable microorganisms that exert beneficial effects on host physiological health when administered at appropriate doses [15]. Accumulating studies have confirmed that functional probiotics can promote growth performance, enhance intestinal immune function, regulate intestinal microecological homeostasis, and inhibit pathogenic bacterial colonization, thereby reducing antibiotic dependence and improving aquaculture economic benefits [16–18]. Excellent intestinal adhesion ability, environmental adaptability and stable colonization capacity are core prerequisites for screening efficient aquaculture probiotics [19]. Therefore, screening and characterizing high-efficiency, safe and host-adaptable probiotic resources has become a key direction for sustainable mariculture research.

The genus *Exiguobacterium* (Bacillaceae) is a group of widely distributed environmental bacteria, commonly isolated from soil, marine sediments, seawater, and extreme habitats including glaciers and alkaline lakes [20–24]. Bacteria of this genus possess flexible metabolic pathways and strong stress resistance, enabling them to tolerate wide variations in temperature, pH and salinity [22]. Notably, *Exiguobacterium* strains exhibit multiple probiotic-related properties, including the capability to secrete extracellular proteases, amylases and lipases, as well as potent antioxidant activity and host surface adhesion ability [23, 25–28]. These functional characteristics endow this genus with great application potential in regulating host nutrient metabolism and improving disease resistance. Existing practical studies have verified the aquaculture application value of *Exiguobacterium* strains: *E. acetylicum* G1-33 isolated from hybrid grouper and *E. arabatum* SB2-5 screened from shrimp gut have been shown to improve the growth performance of aquatic hosts, confirming the probiotic potential of the genus in aquaculture [29, 30]. However, most previous studies have focused on single-host verification, and relatively few have characterized indigenous *Exiguobacterium* strains with stable adaptability and beneficial functions across multiple marine cultured species. Host-derived indigenous strains tend to show better intestinal compatibility and colonization capacity than exogenous probiotics, which may make cross-host indigenous strains particularly valuable for developing universal and sustainable aquaculture probiotics.

In this study, two highly homologous strains, AC31 and R27, were isolated from the intestines of *A. japonicus* and *R. philippinarum*, respectively. Molecular phylogenetic and whole-genome comparative analyses indicated that both isolates belong to a single *Exiguobacterium* strain. The representative strain AC31 was then comprehensively characterized for its phenotypic probiotic traits, biosafety, cross-host growth-promoting effects, and genomic functional mechanisms. Collectively, this study may help elucidate the cross-species probiotic potential of indigenous *Exiguobacterium* strain AC31, offering a promising functional probiotic candidate and a theoretical

basis for the green, sustainable cultivation of sea cucumbers and clams.

Materials and Methods

Isolation of culturable bacteria from the intestinal tracts of *Apostichopus japonicus* and *Ruditapes philippinarum*

Healthy individuals of *A. japonicus* (125.7 ± 13.6 g) and *R. philippinarum* (14.5 ± 1.2 g) were collected in September 2023 and January 2025, respectively, from aquaculture farms in Dalian, Liaoning Province, China. Under sterile conditions, the body surface of each animal was thoroughly rinsed with sterile seawater, after which the intestinal tracts were dissected. Following gentle extrusion of the intestinal contents, the intestinal tracts were rinsed three times with sterile seawater, homogenized on ice, and serially diluted with sterile seawater to 10^{-4}, 10^{-5}, and 10^{-6}. Aliquots (100 μL) were spread onto 2216E agar plates and incubated upside down at 30 ℃ for 24 h. Morphologically distinct colonies were purified by repeated streaking and preserved in 25% (v/v) glycerol at -80 ℃ for subsequent experiments.

In vitro screening of protease-, amylase- and lipase-producing strains

For enzymatic activity screening, overnight cultures were spot-inoculated onto skim milk agar (10 g/L skim milk powder, 10 g/L peptone, 5 g/L yeast extract, 10 g/L NaCl, 15 g/L agar), starch agar (10 g/L soluble starch, 10 g/L peptone, 10 g/L NaCl, 3 g/L beef extract, 15 g/L agar), and Tween 80 agar (10 mL/L Tween 80, 10 g/L peptone, 15 g/L NaCl, 0.1 g/L $CaCl_2$, 15 g/L agar). All plates were incubated upside down at 30 ℃ for 48 h. Hydrolysis zones on skim milk agar and Tween 80 agar indicated protease and lipase activity, respectively; amylase activity was visualized by iodine staining on starch agar.

Hemolysis assay

The hemolytic activity of the enzyme-producing bacterial isolates was evaluated using the blood agar plate method [31]. Overnight cultures were spot-inoculated onto Columbia blood agar plates (Hope Bio-Technology Co., Ltd., Qingdao, China) and incubated upside down at 37 ℃ for 24 h. Isolates showing greenish zones, clear transparent zones, or no surrounding changes were classified as α-, β-, or γ-hemolytic, respectively [32].

Determination of OD-CFU standard curve and growth curve

The target strain was pre-cultured overnight in 2216E broth at 30 ℃ with shaking at 120 rpm. For the OD–CFU standard curve, serial dilutions were measured at OD_{600} and spread onto 2216E agar for CFU counting; linear regression was performed between OD_{600} and bacterial concentration. For the growth curve, 1 mL of overnight culture was inoculated into 100 mL fresh 2216E broth and incubated at 30 ℃ with shaking at 120 rpm, with OD_{600} measured every 4 h.

Bacterial challenge experiment

Healthy *A. japonicus* (3.0-7.0 g) were collected in October 2023 from a commercial hatchery in Dalian, acclimated in 330 L plastic barrels containing 300 L filtered seawater at 20 ± 2 ℃ for one week, and randomly assigned to two groups with three replicates (200 individuals per replicate). The experimental group received the target strain at 1×10^8 CFU/mL, while the control received no

bacterial treatment. Individuals were fed daily at 5% of body weight; morbidity and mortality were recorded daily.

Healthy *R. philippinarum* juveniles (0.141 ± 0.044 g) were collected in November 2025 from the Northern Shellfish Breeding Base of Dalian Ocean University (Yingkou, Liaoning), acclimated in 10 L filtered and disinfected seawater at 20 ± 2 ℃ for seven days, and randomly divided into five groups with three replicates (50 individuals per replicate). Four concentration gradients (1×10^6, 1×10^7, 1×10^8, and 1×10^9 CFU/mL) were applied to experimental groups, whereas the control remained untreated. *Chlorella* was supplied daily, complete water exchange was performed every two days, and corresponding bacterial suspensions were replenished. Mortality was recorded daily.

Culture Experiment of *A. japonicus* and *R. philippinarum* with the target strain

Healthy juvenile *A. japonicus* (2.0-2.5 g) were collected in March 2024 from a commercial hatchery in Dalian; juvenile *R. philippinarum* were obtained from the same batch as in the challenge experiment. After one week of acclimation, individuals of each species were randomly assigned to control and bacterial treatment groups with three biological replicates. *A. japonicus* were cultured in six 330 L plastic barrels containing 300 L filtered seawater (100 individuals per barrel), and *R. philippinarum* in six disinfected 20 L polyethylene tanks filled with 10 L filtered seawater (50 individuals per tank). Water temperature was maintained at 20 ± 2 ℃ with continuous aeration; sterile cotton pads were provided as attachment substrates for *A. japonicus*.

The bacterial suspension was prepared based on the OD–CFU standard curve. Overnight culture was centrifuged at 6000 × g for 5 min, and the pellet was resuspended in sterile seawater. The suspension was added to achieve final concentrations of 1×10^6 CFU/mL for *A. japonicus* and 1×10^7 CFU/mL for *R. philippinarum*; no bacterial suspension was added to controls.

The feeding trial lasted 60 days. *A. japonicus* were fed a standard formulated diet daily at 5% of total whole wet weight, and *R. philippinarum* were fed *Chlorella* once daily. For *A. japonicus*, full water exchange was performed every 10 days, with individual counting and whole wet weight measurement conducted simultaneously and bacterial suspension replenished to 1×10^6 CFU/mL. For *R. philippinarum*, complete water exchange and survival counting were carried out every three days; shell length, shell width, shell height, and whole wet weight were measured on days 15, 30, 45, and 60, and bacterial suspension was replenished to 1×10^7 CFU/mL after each water exchange. At the end of the trial, surviving individuals and whole wet weight were recorded for both species, and shell dimensions were additionally measured for *R. philippinarum*. Survival rate (SR), weight gain rate (WGR), specific growth rate (SGR), and coefficient of variation in body weight (CV) were calculated for both species, whereas shell length gain rate (SLGR), shell width gain rate (SWGR), and shell height gain rate (SHGR) were calculated only for *R. philippinarum*. Formulas (1)-(3) were applied only to *R. philippinarum*, whereas Formulas (4)-(7) were applied to both species.

$$SLGR(\%) = \frac{L_t - L_0}{L_0} \times 100 \quad (1)$$

$$SWGR(\%) = \frac{W_t - W_0}{W_0} \times 100 \quad (2)$$

$$\mathrm{SHGR}(\%) = \frac{\mathrm{H_t} - \mathrm{H_0}}{\mathrm{H_0}} \times 100 \quad (3)$$

$$\mathrm{WGR}\ (\%) = \frac{m_t - m_0}{m_0} \times 100 \quad (4)$$

$$\mathrm{SR}\ (\%) = \frac{\mathrm{n_t}}{\mathrm{n_0}} \times 100 \quad (5)$$

$$\mathrm{SGR}\ (\%\ d^{-1}) = \frac{\ln m_t - \ln m_0}{\mathrm{t}} \times 100 \quad (6)$$

$$\mathrm{CV}\ (\%) = \left(\frac{\mathrm{SD}}{\mathrm{X}}\right) \times 100 \quad (7)$$

where L_0 and L_t, B_0 and B_t, and H_0 and H_t represent the initial and final mean shell Len glen, shell widths, and shell heights (mm), respectively; n_0 represents the initial individual number, n_t represents the final individual number, m_0 indicates the initial mean whole wet weight, m_t indicates the final mean whole wet weight, t is the total rearing duration (day s), SD is the standard deviation, and X is the average whole wet weight.

Morphological characterization and 16S rRNA-based molecular identification

Colonial morphology was observed on 2216E agar, and Gram staining was performed using a commercial kit (Solarbio, Beijing, China). Cell morphology and size were characterized by scanning electron microscopy (SEM; ZEISS Sigma 360, Jena, Germany).

Bacterial genomic DNA was extracted by the boiling-lysis method [33]. The 16S rRNA gene was amplified with primers 27F (5'-GAGTTTGATCCTGGCTCAG-3′) and 1492R (5'-GGTTACCTTGTTACGACTT-3′). The 30 μL PCR reaction contained 1 μL of each primer, 15 μL 2 × Rapid Taq Master Mix, 1 μL DNA template, and 12 μL ddH2O. Thermal cycling was: initial pre-denaturation at 95 ℃ for 2 min; 35 cycles of 98 ℃ for 10 s, 55 ℃ for 30 s, and 68 ℃ for 2 s; final extension at 68 ℃ for 5 min. Amplicons were checked by 1.5% agarose gel electrophoresis and Sanger-sequenced by BGI Genomics (Shenzhen, China). Sequences were aligned using NCBI BLAST (https://blast.ncbi.nlm.nih.gov/). A phylogenetic tree was constructed in MEGA 12.0 using the neighbor-joining algorithm with 1500 bootstrap replicates, with *Bacillus subtilis* as the outgroup.

Whole-genome sequencing, functional annotation and average nucleotide identity (ANI) analysis

Genomic DNA was extracted using the E.Z.N.A. Bacterial DNA Kit (OMEGA, Georgia, USA). Whole-genome sequencing was performed on Illumina MiSeq and PacBio Sequel platforms. For Illumina sequencing, genomic DNA was fragmented using a Covaris system, and libraries were prepared by standard procedures (end repair, adapter ligation, PCR amplification, and quality control) followed by paired-end sequencing. For PacBio sequencing, genomic DNA was processed into 8–10 kb fragments using the G-tube method, end-repaired, ligated with SMRTbell adapters to construct circular libraries, annealed to sequencing primers, bound to polymerase, and sequenced on the PacBio Sequel platform.

Gene prediction was performed using GeneMark (http://topaz.gatech.edu/GeneMark/). Predicted protein sequences were aligned against NCBI Non-Redundant Database (NR), SwissProt (http://uniprot.org), KEGG (http://www.genome.jp/kegg/), GO (http://www.geneontology.org/), COG (http://www.ncbi.nlm.nih.gov/COG), CAZy (http://www.cazy.org/), CARD (https://card.mcmaster.ca), PHI, TCDB (http://www.tcdb.org/), VFDB, BacMet, SignalP (http://www.cbs.dtu.dk/services/SignalP/), and TMHMM (http://www.cbs.dtu.dk/services/TMHMM/) using BLASTP. tRNA and rRNA genes were identified using tRNAscan-SE (v2.0.4, http://lowelab.ucsc.edu/tRNAscan-SE) and RNAmmer (v1.2,

http://www.cbs.dtu.dk/services/RNAmmer/), respectively.

ANI values were calculated among the target strains and 18 representative related strains with complete genomes (Table 1) through pairwise genome alignment based on the ANI-Blast (ANIb) algorithm implemented in JSpeciesWS (https://jspecies.ribohost.com/).

Table 1 Information of genomes used in ANI analysis

Species	Strain	Version or Accession no.
Exiguobacterium sibiricum	255-15	CP001022.1
Exiguobacterium chiriqhucha	RW-2	ATCL01000001.1
Exiguobacterium undae	DSM 14481	KK211187.1
Exiguobacterium marinum	DSM 16307	KK211189.1
Exiguobacterium antarcticum	DSM 14480	JMKS01000001.1
Exiguobacterium aurantiacum	DSM 6208	JNIQ01000001.1
Exiguobacterium oxidotolerans	JCM 12280	JNIS01000001.1
Exiguobacterium indicum	HHS 31	MPSZ01000001.1
Exiguobacterium flavidum	HF60	QPKS01000001.1
Exiguobacterium sp.	TBG-PICH-001	JADOYC010000008.1
Exiguobacterium alkaliphilum	B-3531D	CP073101.1
Exiguobacterium acetylicum	SI17	CP075897.1
Exiguobacterium qingdaonense	S82	JACSKY010000001.1
Exiguobacterium algae	S126	JACSKZ010000001.1
Exiguobacterium himgiriensis	K22_26	JANIEI010000092.1
Exiguobacterium mexicanum	IMTB_3094	JANIEJ010000019.1
Exiguobacterium profundum	CGMCC 4.7397	JBHSHG010000001.1
Exiguobacterium aestuarii	CGMCC 1.16590	JBHSZW010000001.1

Phenotypic metabolic profiling and antimicrobial susceptibility assay

Metabolic characteristics were analyzed using the Biolog GEN III Microplate system (Biolog Inc., CA, USA), with plate reading and data analysis performed using MicroStation and Microbial Identification Systems software.

Antibiotic susceptibility was determined by the Kirby–Bauer disc diffusion method [34]. A 100 μL standardized bacterial suspension was spread onto 2216E agar plates, sterile antibiotic discs were placed on the agar surface, and plates were incubated at 30 ℃ for 48 h. Inhibition zone diameters were measured with a Vernier caliper. All experiments were performed in triplicate. Results were classified as sensitive (S), intermediate (I), or resistant (R) according to CLSI 2010 criteria.

Acid and bile salt tolerance assays

Bile tolerance was assessed by inoculating 2% (v/v) freshly cultured suspension into 2216E liquid medium supplemented with bile salts (Aladdin Biochemical Technology Co., Ltd., Shanghai, China) at 0%, 0.1%, 0.3%, 0.5%, and 0.7% (w/v). Cultures were incubated at 30 ℃ with shaking at 120 rpm for 24 h, and OD600 was recorded. All assays were performed in triplicate. Survival rate (W, %) was calculated as:

$$W = \frac{A_1}{A_0} \times 100\% \quad (8)$$

where A_0 is the OD_{600} of the untreated control, and A_1 is the OD_{600} of the treated sample after

incubation.

pH tolerance was evaluated by inoculating 2% (v/v) freshly cultured suspension into 2216E liquid medium adjusted to pH 3.0, 4.0, 5.0, 6.0, and 7.0 with 0.1 mol/L HCl and 0.1 mol/L NaOH. Cultures were incubated at 30 ℃ with shaking at 120 rpm for 24 h, and OD600 was measured. All assays were performed in triplicate. Survival rate (W, %) was calculated as:

$$W = \frac{A_1}{A_0} \times 100\% \quad (9)$$

where A_0 is the OD_{600} of the untreated control, and A_1 is the OD_{600} of the treated sampl e after incubation.

Extracellular enzyme activity assays

α-amylase and lipase activities were determined using commercial assay kits from Nanjing Jiancheng Bioengineering Institute (Nanjing, China) according to the manufacturer's instructions. Protease activity was measured using a commercial assay kit from Suzhou Grace Biotechnology Co., Ltd. (Suzhou, China). The cell-free fermentation supernatant was used for all enzyme activity determinations.

One unit (U) of α-amylase activity was defined as the amount of enzyme catalyzing the production of 1 mg reducing sugar per mL of sample per minute. One unit of lipase activity was defined as the amount of enzyme consuming 1 μmol substrate per minute at 37 ℃. One unit of protease activity was defined as a change of 1 absorbance unit in the reaction system per mL of sample per hour. All enzyme activities are expressed as U/mL in the Results section, with lipase activity converted from U/L to U/mL. All assays were performed in triplicate.

Antioxidant capacity evaluation

DPPH radical scavenging activity was assessed according to Pisu et al. [35] with slight modifications. Briefly, 2 mL cell-free fermentation supernatant was mixed with 2 mL DPPH methanolic solution (0.2 mM) and incubated at 25 ℃ in the dark for 30 min, after which absorbance was measured at 517 nm. Trolox was used as the positive control. In the blank group, an equal volume of ethanol replaced the DPPH solution; in the control group, an equal volume of distilled water replaced the sample. An equal volume of distilled water-absolute ethanol mixture was used for zero calibration. All assays were performed in triplicate. DPPH free radical scavenging rate was calculated as:

$$\text{DPPH free radical scacenging rate } (\%) = [1 - \frac{(A_1 - A_0)}{A_2}] \times 100 \quad (10)$$

where A_0 is the absorbance of the blank group, A_1 is the absorbance of the sample group, and A_2 is the absorbance of the control group.

ABTS radical scavenging capacity was determined based on Zhang et al. [36] with slight modifications. The working solution was prepared by mixing equal volumes of 7 mM ABTS and 2.45 mM potassium persulfate, incubated in the dark for 12 h, and diluted to an absorbance of 0.70 ± 0.02 at 734 nm before use. Briefly, 0.2 mL sample was added to 0.8 mL diluted working solution and incubated at 25 ℃ in the dark for 10 min, after which absorbance was measured at 734 nm. Trolox was used as the positive control. An equal volume of water replaced the sample as the blank control. All assays were performed in triplicate. ABTS free radical scavenging rate was calculated as:

$$\text{ABTS free radical scacenging rate (\%)} = \left(1 - \frac{A_1}{A_0}\right) \times 100 \quad (11)$$

where A_0 is the absorbance of the control group, and A_1 is the absorbance of the sample group.

In vitro auto-aggregation and adhesion ability assays

Cell-surface hydrophobicity was evaluated using the xylene extraction method according to Long et al. [37]. Briefly, bacterial suspension (prepared in PBS, OD_{600} = 1.0) was mixed 1:1 (v/v) with xylene, chloroform, and ethyl acetate, respectively, vortexed for 5 min, and incubated statically at 25 ℃ for 30 min. The aqueous phase was collected for hydrophobicity determination at OD_{600}. All assays were performed in triplicate. Hydrophobicity was calculated as:

$$\text{Hydrophobicity(\%)} = \left(1 - \frac{A_1}{A_0}\right) \times 100 \quad (12)$$

where A_0 is the initial absorbance of the target strain before mixing, and A_1 is the absorbance of the aqueous phase after mixing.

Auto-aggregation ability was assessed following Kumari et al. [38] with slight modifications. The bacterial suspension was incubated statically at 25 ℃, and the absorbance of the upper layer was measured at OD600 after 2, 4, 6, 8, 12, and 24 h. All assays were performed in triplicate. Auto-aggregation rate was calculated as:

$$\text{Autoaggregation(\%)} = \left(1 - \frac{A_1}{A_0}\right) \times 100 \quad (13)$$

where A_0 is the initial absorbance of the target strain, and A_1 is the absorbance at time = 2, 4, 6, 8, 12 or 24 h.

Intestinal colonization potential assessment

A. japonicus and *R. philippinarum* individuals were collected 24 h after strain administration. Before dissection, the body surface was rinsed thoroughly with sterile seawater to minimize external contamination. Intestinal tissues were aseptically dissected and homogenized in PBS. For short-term enrichment, aliquots of intestinal homogenates were inoculated into 2216E liquid medium and incubated at 30 ℃ for 12 h. After enrichment, bacterial cells were collected by centrifugation, and genomic DNA was extracted using the TIANamp Bacteria DNA Kit (TIANGEN Biotech, Beijing, China). The target strain was detected by conventional PCR using a specific primer pair targeting the *cytc550* gene (F 5'-GGCGTAAACCAAGCACAAC-3′; R 5'-GACACCAGTCAAGGCAGGA-3′). PCR products were analyzed by agarose gel electrophoresis, and the presence of an amplicon of the expected size was considered positive detection of the target strain in the enriched intestinal samples.

Animal experiments and ethical approval statement

Ethical review and approval were waived for this study, as *A. japonicus* and *R. philippinarum* are invertebrates.

Statistical analysis

Statistical analyses were performed using R (v4.5.2). Data are presented as the mean ± SD. Differences between two groups were assessed using Student's *t*-test, whereas differences among multiple groups were assessed by one-way analysis of variance (ANOVA) followed by Tukey's

multiple-comparison test. Statistical significance was defined as $P < 0.05$ (*) and $P < 0.01$ (**).

Results

Isolation and screening of a triple enzyme-producing bacterial strain AC31 from the intestinal tract of *Apostichopus japonicus*

Potential probiotic strains were isolated from the intestinal tracts of healthy *A. japonicus*, yielding a total of 37 culturable bacterial isolates. All isolates were initially screened for extracellular protease, amylase, and lipase production. Among them, 15 isolates were protease-positive, 20 were amylase-positive, and 8 were lipase-positive, while 8 isolates exhibited no detectable activity for any of the three enzymes (Table S1). Of the enzyme-producing strains, twelve produced two enzymes and one produced three enzymes. Hemolysis testing of the strains producing two or three enzymes revealed that, except for two strains producing two enzymes, the remaining 11 strains did not form β-hemolytic rings (Table S1). Consequently, the triple enzyme-producing strain AC31 was selected for further investigation. The *in vitro* protease, amylase, and lipase production capabilities of this strain are illustrated in Fig. 1A-C, and the hemolysis assay result is presented in Fig. 1D.

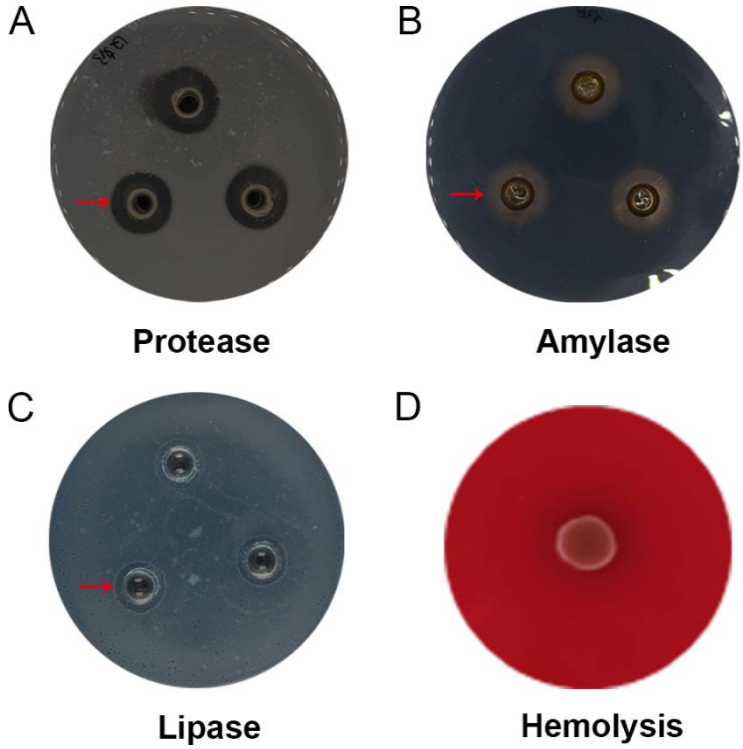


Fig. 1 Extracellular digestive enzyme producing and hemolytic phenotypes of strain AC31. (A) Protease production. (B) Amylase production. (C) Lipase production. White arrows indicate the hydrolysis zones surrounding the colonies. (D) Hemolytic phenotype on blood agar.

The bacterial OD-CFU standard curve and growth curve of strain AC31

To facilitate the quantification of strain AC31, an OD-CFU standard curve was established. As shown in Fig. 2A, the OD_{600} values exhibited a strong linear relationship with CFU counts (R^2=0.9975), indicating that optical density measurements could reliably reflect colony-forming units. Based on the growth curve of strain AC31 in 2216E broth at 30 ℃ and 120 rpm, a lag phase was observed from 0 h to 8 h, followed by an exponential phase from 8 h to 24 h. A stationary phase

occurred from 24 h to 36 h, and a decline phase was observed after 36 h (Fig. 2B).

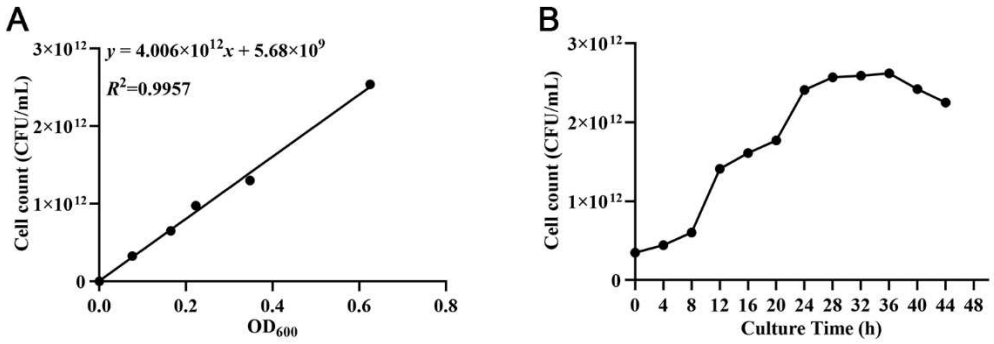


Fig. 2 The OD-CFU standard curve (A) and growth curve (B) of strain AC31

Bacterial challenge of *A. japonicus* with strain AC31

To evaluate the safety of strain AC31 for probiotic application, its acute toxicity to *A. japonicus* was assessed by an immersion challenge experiment. Based on the LD_{50} of *Vibrio splendidus* in *A. japonicus* reported by Li et al. (2010) (1.74×10^7 CFU/g body weight)[39], a challenge concentration of 10^8 CFU/mL was selected to ensure sufficient infection pressure to reveal any potential toxicity of strain AC31. As shown in Table 2, the survival rate of *A. japonicus* exposed to AC31 at 1×10^8 CFU/mL was 99.5 ± 0.41%, which was significantly higher than that of the control group (96.8 ± 0.62%; $P < 0.05$). No increase in mortality was observed after AC31 exposure, indicating that AC31 caused no detectable acute mortality in *A. japonicus* under the tested conditions.

Table 2 Acute safety assessment of strain AC31 in *A. japonicus*

Group	Initial number of *A. japonicus*	Number of survivors (Day 7)	Survival rate (%)
Control	200	193 ± 1.25	96.8 ± 0.62^b
AC31 (1×10^8 CFU/mL)	200	199 ± 0.82	99.5 ± 0.41^a

Note: Values with the difference letters are significantly different ($P < 0.05$).

Growth performance of *A. japonicus* in the culture experiment with strain AC31

To evaluate the effects of chronic dietary supplementation with AC31 on the survival and growth of *A. japonicus* under aquaculture conditions, a 60-day feeding trial was conducted. Throughout the experimental period, the survival rate of the AC31-supplemented group remained above 95% and did not differ significantly from that of the control group at any sampling time point ($P > 0.05$; Fig. 3). No abnormal mortality or observable adverse responses were recorded during the trial, indicating that dietary supplementation with AC31 did not adversely affect the survival of *A. japonicus* under the tested conditions.

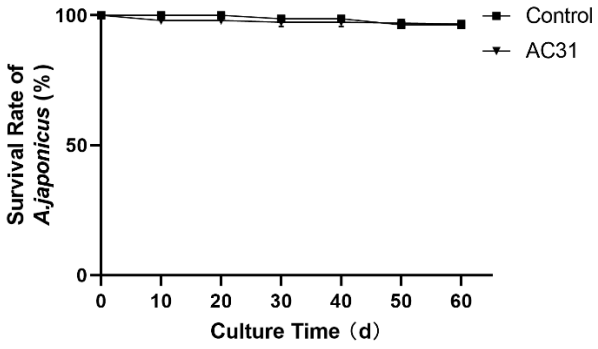


Fig. 3 Survival rates of *A. japonicus* in the control group and the AC31-supplemented group during the 60-day culture period.

After 60 days, the mean body weight of *A. japonicus* increased from 2.18 ± 0.10 g to 2.87 ± 0.05 g in the AC31-supplemented group and from 2.37 ± 0.09 g to 2.95 ± 0.05 g in the control group. In the AC31-supplemented group, both the weight gain rate and specific growth rate were significantly higher than those in the control group ($P < 0.05$; Table 3). Additionally, the coefficient of variation (CV) of weight was slightly lower in the AC31-supplemented group, suggesting a tendency toward greater size uniformity.

Table 3 Growth performance of *A. japonicus* in the culture experiment

Group	Initial average weight (g)	Final average weight (g)	Weight gain rate (%)	Specific growth rate (% d^{-1})	CV of weight (%)
Control	2.37 ± 0.09	2.95 ± 0.05	24.37 ± 2.09^{b}	0.36 ± 0.03^{b}	1.68
AC31 (1×10^{6} CFU/mL)	2.18 ± 0.10	2.87 ± 0.05	31.68 ± 2.15^{a}	0.46 ± 0.03^{a}	1.63

Notes: Values are presented as mean ± SD (n = 3). Within each column, values with different superscript lowercase letters indicate significant differences among groups ($P < 0.05$). Statistical comparisons were performed only among groups within the same parameter; no comparisons were made among different parameters.

Morphological characteristics and 16S rRNA gene-based molecular identification of strain AC31

Colonies of AC31 grown on 2216E agar plates were opaque, orange-yellow and circular with smooth margins (Fig. 4A). Gram staining produced a purple coloration, indicating that strain AC31 is Gram-positive (Fig. 4B). Scanning electron microscopy (SEM) revealed that strain AC31 cells were spherical to ovoid, with a rough, irregular surface exhibiting a granular to reticulated texture (Fig. 4C). The cells were closely packed and aggregated, and filamentous surface-associated structures were observed on some cells (Fig. 4C). The 16S rRNA gene sequence of AC31 was deposited in GenBank under accession number PX401721. Phylogenetic analysis based on 16S rRNA gene sequences placed strain AC31 within the genus *Exiguobacterium* and showed that it clustered closely with *E. aurantiacum* strain P107-DB-C5 (Fig. 4D).

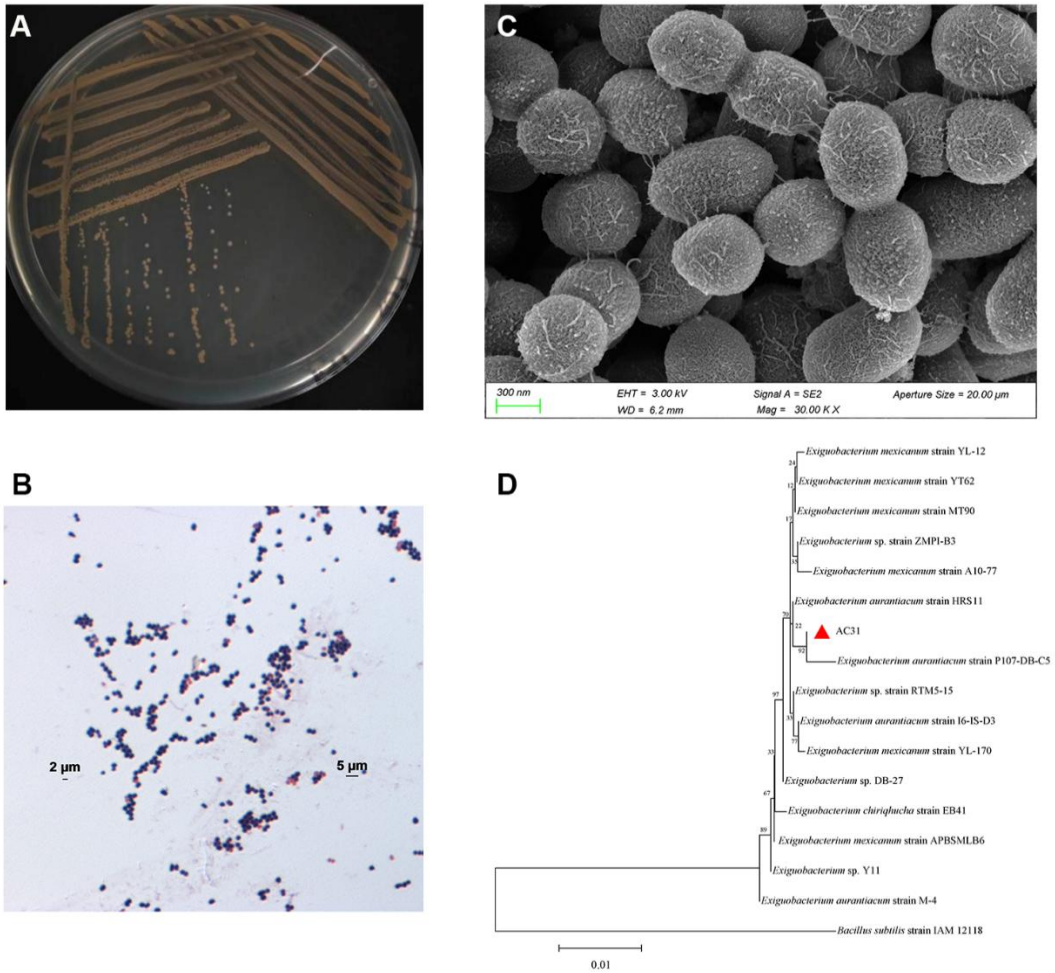


Fig. 4 Morphology and molecular identification of strain AC31. (A) Colonies of strain AC31 on 2216E medium. (B) Gram staining. (C) Scanning electron microcopy (SEM). (D) Phylogenetic tree.

Whole-genome properties and ANI-based taxonomic identification of strain AC31

To further resolve the taxonomic position of strain AC31 and to better understand its genomic architecture and functional potential, whole-genome sequencing was performed, yielding 308,336 reads. The complete genome sequence has been deposited in GenBank under accession number JBYLET000000000. The assembled genome was 3,092,758 bp in length and comprised one circular chromosome (Fig. 5A) and one circular plasmid (Fig. 5B). It had a GC content of 51.77% and contained 3,201 coding genes with a total length of 2,747,166 bp and an average length of 858 bp. The coding genes accounted for 88.8% of the total genome length. The genome comprised 28 rRNAs and 67 tRNAs.

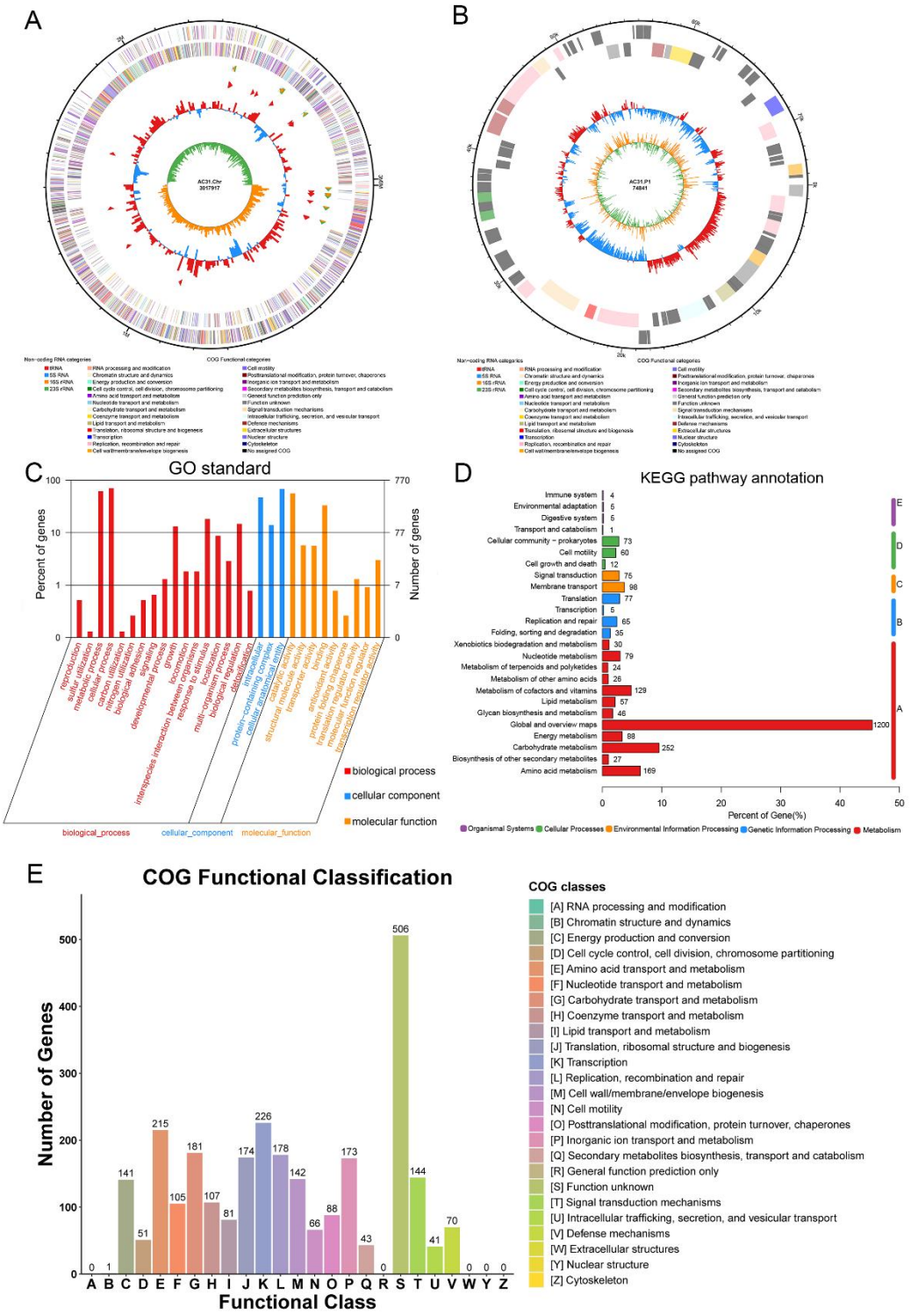


Fig. 5 Whole genome feature analysis and functional annotation of strain AC31. Genome circle maps of (A) the chromosome and (B) the plasmid. Distribution of annotated genes across functional categories in the (C) GO, (D) KEGG, and (E) eggNOG databases. In the genome circle maps, the outermost circle indicates the genome size, while the second and third circles represent coding sequences (CDSs) on the forward and reverse strands, respectively, with colors denoting different COG functional categories. The fourth circle shows the distribution of rRNA and tRNA genes, and the fifth circle depicts the GC content. Regions extending outward in red indicate a GC content

above the genome-wide average, whereas regions facing inward in blue indicate a GC content below the average value, with the magnitude of deviation reflected by the peak heights. The innermost circle represents the GC skew, calculated as (G − C)/(G + C). Positive values indicate a higher likelihood of CDSs being transcribed from the forward strand, while negative values indicate transcription from the reverse strand.

Genome-level ANI analysis further supported the assignment of strain AC31 to *Exiguobacterium chiriqhucha*. Strain AC31 exhibited an ANI value of 95.98% with the reference genome of *E. chiriqhucha*, exceeding the widely accepted species delineation threshold of 95% [40]. Therefore, although strain AC31 clustered with *E. aurantiacum* in the 16S rRNA gene-based phylogenetic tree, whole-genome ANI analysis supported its classification as *E. chiriqhucha* (Fig. 6). This discrepancy may reflect the higher taxonomic resolution of genome-wide comparisons than that of 16S rRNA gene sequence analysis for distinguishing closely related species.

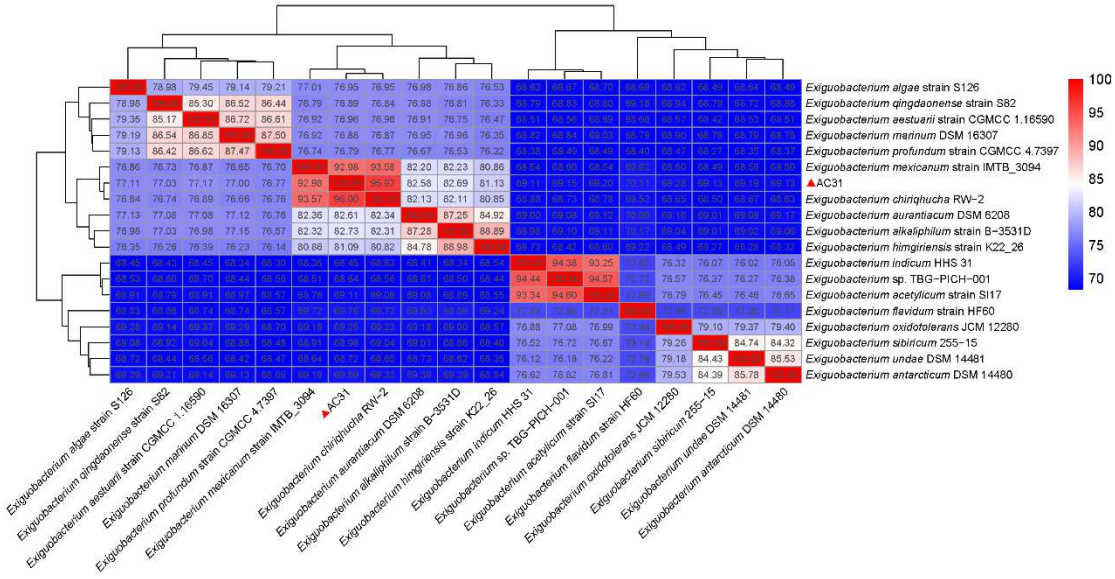


Fig. 6 ANI analysis based on whole-genome comparisons among different strains of *Exiguobacterium*.

Metabolic profiles and antibiotics resistance of strain AC31

Biolog GEN III MicroPlate-based metabolic profiling revealed that strain AC31 could utilize a wide range of carbon substrates, including polysaccharides (dextran), monosaccharides and amino sugars (α-D-glucose, N-acetyl-β-D-mannosamine), proteins (gelatin), organic acids (L-lactic acid, acetoacetate, sodium butyrate), as well as inorganic salts (lithium chloride), demonstrating the broad metabolic versatility of strain AC31 (Table 4).

Table 4 Metabolic profiles of strain AC31 using Biolog Gen III microplate

Well	Reaction item	Result	Well	Reaction item	Result
A1	Negative Control	-	E1	Gelatin	+
A2	Dextrin	+	E2	Glycyl-L-Proline	-
A3	D-Maltose	w	E3	L-Alanine	w
A4	D-Trehalose	w	E4	L-Arginine	-
A5	D-Cellobiose	-	E5	L-Aspartic Acid	-
A6	Gentiobiose	w	E6	L-Glutamic Acid	-
A7	Sucrose	w	E7	L-Histidine	-
A8	D-Turanose	-	E8	L-Pyroglutamic Acid	-

A9	Stachyose	-	E9	L-Serine	w
A10	Positive Control	+	E10	Lincomycin	w
A11	pH 6	w	E11	Guanidine HCl	w
A12	pH 5	-	E12	Niaproof 4	-
B1	D-Raffinose	-	F1	Pectin	w
B2	α-D-Lactose	-	F2	D-Galacturonic Acid	-
B3	D-Melibiose	-	F3	L-Galactonic Acid Lactone	-
B4	β-Methyl-D Glucoside	w	F4	D-Gluconic Acid	w
B5	D-Salicin	w	F5	D-Glucuronic Acid	-
B6	N-Acetyl-D Glucosamine	w	F6	Glucuronamide	w
B7	N-Acetyl-β-D Mannosamine	+	F7	Mucic Acid	-
B8	N-Acetyl-D Galactosamine	-	F8	Quinic Acid	-
B9	N-Acetyl Neuraminic Acid	-	F9	D-Saccharic Acid	-
B10	1% NaCl	+	F10	Vancomycin	-
B11	4% NaCl	+	F11	Tetrazolium Violet	w
B12	8% NaCl	w	F12	Tetrazolium Blue	w
C1	α-D-Glucose	+	G1	p-Hydroxy-Phenylacetic Acid	-
C2	D-Mannose	-	G2	Methyl Pyruvate	-
C3	D-Fructose	w	G3	D-Lactic Acid Methyl Ester	-
C4	D-Galactose	-	G4	L-Lactic Acid	+
C5	3-Methyl Glucose	-	G5	Citric Acid	-
C6	D-Fucose	-	G6	α-Keto-Glutaric Acid	-
C7	L-Fucose	-	G7	D-Malic Acid	-
C8	L-Rhamnose	-	G8	L-Malic Acid	-
C9	Inosine	w	G9	Bromo-Succinic Acid	-
C10	1% Sodium Lactate	w	G10	Nalidixic Acid	w
C11	Fusidic Acid	-	G11	Lithium Chloride	+
C12	D-Serine	-	G12	Potassium Tellurite	w
D1	D-Sorbitol	-	H1	Tween 40	-
D2	D-Mannitol	w	H2	γ-Amino-Butryric Acid	-
D3	D-Arabitol	-	H3	α-Hydroxy-Butyric Acid	-
D4	myo-Inositol	-	H4	β-Hydroxy-D, L-butyric Acid	-
D5	Glycerol	w	H5	α-Keto-Butyric Acid	-
D6	D-Glucose-6-PO4	-	H6	Acetoacetic Acid	+
D7	D-Fructose-6-PO4	w	H7	Propionic Acid	-
D8	D-Aspartic Acid	-	H8	Acetic Acid	w

D9	D-Serine	-	H9	Formic Acid	-
D10	Troleandomycin	w	H10	Aztreonam	-
D11	Rifamycin SV	-	H11	Sodium Butyrate	+
D12	Minocycline	-	H12	Sodium Bromate	w

Note: "+" represents positive result, "–" represents negative result, "w" represents weakly positive result. Negative control: A1; positive control: A10; carbon source utilization: 1-9; chemical sensitivity: D, E, F, G, H 10-12; environmental factors: A, B, C 10-12.

Furthermore, strain AC31 exhibited diverse antibiotic susceptibility. Based on standardized breakpoints, the strain was highly susceptible to multiple clinically important antibiotics, including rifampicin, amoxicillin, cefalexin and tetracycline. In contrast, strain AC31 was resistant to kanamycin, erythromycin, ciprofloxacin and azithromycin. It also showed intermediate susceptibility to clindamycin, norfloxacin and neomycin. Full interpretations of antibiotic susceptibility, together with the corresponding inhibition zone diameters, are summarized in Table 5.

Table 5 Antibiotic susceptibility of strain AC31

Name of antibiotic	Criteria based on diameter of inhibitory zone (mm)			Inhibitory zone diameter of strain AC31 (mm)	Sensitivity
	Resistant (R)	Intermediate (I)	Susceptible (S)		
Rifampicin	≤16	17~18	≥19	26.47 ± 2.67	S
Kanamycin	≤13	14~17	≥18	12.10 ± 0.75	R
Cefalexin	≤14	15~17	≥18	29.97 ± 1.35	S
Erythromycin	≤13	14~22	≥23	12.80 ± 0.15	R
Co-trimoxazole	≤10	11~15	≥16	10.13 ± 0.23	I
Norfloxacin	≤12	13~16	≥17	13.10 ± 0.82	I
Neomycin	≤12	13~16	≥17	15.37 ± 0.55	I
Ciprofloxacin	≤15	16~20	≥21	14.60 ± 0.17	R
Tetracycline	≤14	15~18	≥19	21.13 ± 0.84	S
Furazolidone	≤14	15~16	≥17	17.67 ±0 .70	S
Amoxicillin	≤19	-	≥20	29.52 ± 0.43	S
Azithromycin	≤13	14~17	≥18	0	R
Polymyxin B	≤8	8~11	≥12	0	R
Lincomycin	≤14	15~20	≥21	0	R
Vancomycin	≤9	10~11	≥12	17.23 ± 0.68	S
Streptomycin	≤6	7~9	≥10	0	R
Gentamicin	≤6	7~9	≥10	13.40 ± 0.46	S
Clindamycin	≤14	15~20	≥21	17.03 ± 1.00	I
Chloramphenicol	≤12	13~17	≥18	22.10 ± 1.11	S

Note: "R" represents resistant, "I" represents intermediate, and "S" represent susceptible.

Screening of a triple enzyme-producing bacterial strain R27 with growth-promoting capacity from the intestines of *Ruditapes philippinarum*

A separate experiment was performed to screen potential probiotics for *R. philippinarum*. A total of 53 culturable bacterial isolates were recovered from the intestinal tracts. Consistent with the

screening strategy for *A. japonicus* described above, these isolates were first assessed for enzyme activities, and enzyme-positive isolates were then subjected to hemolysis assays, with results shown in Table S1. Among these isolates, 25 were protease-positive, 27 were amylase-positive, and 9 were lipase-positive. Ten isolates exhibited no detectable activity for any of the three enzymes. One isolate produced all three target enzymes, and 16 isolates produced two of the three tested enzymes. Based on the hemolysis assay results, strain R27 was selected for subsequent characterization and growth-promotion evaluation, as it produced all three target enzymes and lacked β-hemolytic activity. Preliminary experiments demonstrated that strain R27 was not only non-toxic to *R. philippinarum* but also beneficial to its growth (data not shown).

Taxonomic congruence of strains R27 and AC31 based on morphological, molecular, and genomic characteristics

Subsequently, a systematic taxonomic characterization of strain R27 was conducted. Strain R27 shared colony and cellular morphological features with strain AC31. Both strains formed opaque, orange-yellow, circular colonies with smooth edges, and their cells were Gram-positive. Pairwise alignment of 16S rRNA gene sequences revealed >99% sequence similarity between R27 and AC31 (Fig. S1), suggesting a close taxonomic relationship. To determine whether strain R27 was identical to strain AC31, whole-genome sequencing was performed on strain R27, and the circular genome map is presented in Fig. 7. Subsequent whole-genome comparison yielded an ANI value of 100% between the two strains, confirming their genomic identity (Fig. S2). The genome sequence of R27 has been deposited in GenBank under BioSample: SAMN59967034. Collectively, consistent morphological traits, combined with molecular and genomic evidence, demonstrated that strains R27 and AC31 belonged to the same strain. Accordingly, the two designations were merged, and strain AC31 was adopted for all subsequent experiments and analyses.

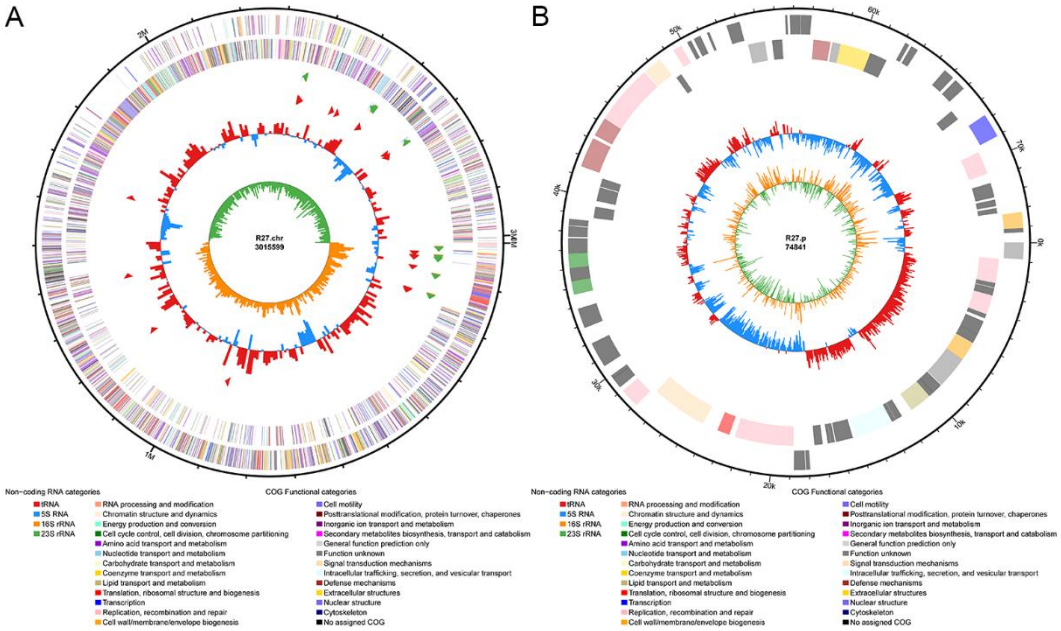


Fig. 7 Whole genome feature analysis and functional annotation of strain R27. Genome circle maps of (A) the chromosome and (B) the plasmid.

Bacterial challenge of *R. philippinarum* with strain AC31

The acute toxicity of strain AC31 toward *R. philippinarum* was first assessed. Clams were exposed via immersion to strain AC31 at concentrations ranging from 1×10^6 to 1×10^9 CFU/mL. As shown in Table 6, survival rates ranged from 99.33 ± 0.94% to 100% across all tested concentrations, and mortality did not differ significantly from that of the control group ($P > 0.05$). These results indicate that AC31 induced no detectable acute mortality in *R. philippinarum* under the tested conditions.

Table 6 Acute safety assessment of strain AC31 in *R. philippinarum*

Group	Initial number of *R. philippinarum*	Number of survivors (Day 7)	Survival rate (%)
Control	50	49 ± 0.47	98.67 ± 0.94[a]
AC31 (1×10^6 CFU/mL)	50	50	100[a]
AC31 (1×10^7 CFU/mL)	50	50	100[a]
AC31 (1×10^8 CFU/mL)	50	49 ± 0.47	99.33 ± 0.94[a]
AC31 (1×10^9 CFU/mL)	50	50	100[a]

Note: Values are presented as mean ± SD (n = 3). Different superscript letters indicate significant differences ($P < 0.05$); the same letter indicates no significant difference.

Growth performance of *R. philippinarum* in the culture experiment with strain AC31

The effects of chronic dietary supplementation with AC31 on the survival and growth of *R. philippinarum* were further investigated in a 60-day feeding trial. The survival rate of the AC31-supplemented group remained above 95% throughout the experimental period and showed no significant difference from that of the control group at any sampling time point ($P > 0.05$; Fig. 8), and no abnormal mortality or obvious adverse reactions were observed, suggesting that dietary AC31 supplementation exerted no negative impact on clam survival under the tested conditions.

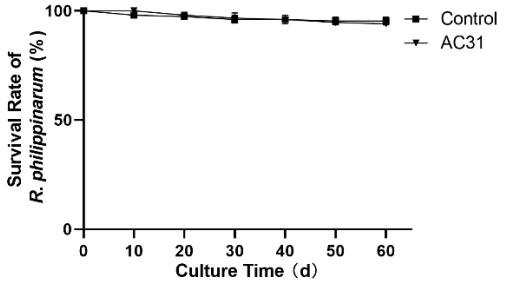


Fig. 8 Survival rates of *R. philippinarum* during the 60 days culture period with AC31 or without AC31 supplementation.

Regarding growth performance, the gain rates of shell length, shell width, and shell height in the AC31-supplemented group were 19.67 ± 0.96%, 26.48 ± 0.98%, and 22.64 ± 1.61%, respectively; average body weight increased from 0.11 ± 0.02 g to 0.18 ± 0.01 g, with a weight gain rate of 63.94 ± 9.57%, a specific growth rate of 0.71 ± 0.10%, and a CV of weight of 5.71%. In comparison, the control group showed shell length, shell width, and shell height growth rates of 13.77 ± 1.00%, 18.28 ± 1.28%, and 14.29 ± 1.12%, respectively; average body weight increased from 0.12 ± 0.03 g to 0.16 ± 0.01 g, with a weight gain rate of 36.67 ± 6.05%, a specific growth rate of 0.52 ± 0.07%,

and a CV of weight of 4.43%. The growth rates of shell length, shell width, and shell height, as well as the weight gain rate and specific growth rate, were all significantly higher than those in the control group ($P < 0.05$), indicating that supplementation with strain AC31 could promote the growth of *R. philippinarum*. In contrast to the observations in *A. japonicus*, clams in the experimental group exhibited a higher CV of weight relative to the control group.

Table 7 Growth performance of *R. philippinarum* in the culture experiment

Group	Shell length gain rate (%)	Shell width gain rate (%)	Shell height gain rate (%)	Initial average weight (g)	Final average weight (g)	Weight gain rate (%)	Specific growth rate (% d^{-1})	CV of weight (%)
Control	13.77 ± 1.00 ^{b}	18.28 ± 1.28 ^{b}	14.29 ± 1.12 ^{b}	0.12 ± 0.03	0.16 ± 0.01	36.67 ± 6.05^{b}	0.52 ± 0.07^{b}	4.43
AC31 (1×10^{7} CFU/mL)	19.67 ± 0.96 ^{a}	26.48 ± 0.98 ^{a}	22.64 ± 1.61 ^{a}	0.11 ± 0.02	0.18 ± 0.01	63.94 ± 9.57^{a}	0.71 ± 0.10^{a}	5.71

Notes: Values are presented as mean ± SD (n = 3). Within each column, values with different superscript lowercase letters indicate significant differences between groups ($P < 0.05$). Statistical comparisons were performed only between groups for the same parameter; no comparisons were made among different parameters.

Stress tolerance, functional activity, and colonization potential of strain AC31

The suitability of strain AC31 as a probiotic for mariculture organisms was further systematically investigated. First, its tolerance to acid and bile salts was evaluated. As shown in Fig. 9A, after 7 days of incubation under acidic conditions, the strain showed an almost complete loss of viability at pH 3-5, with survival rates below 5%. The survival rate rose to approximately 50% at pH 6, whereas the strain retained almost full viability at pH 7. Although approximately 50% of cells survived at pH 6, indicating partial acid tolerance, the strain is unlikely to maintain its activity under low-pH acidic conditions. Likewise, as shown in Fig. 9B, the growth of AC31 was markedly inhibited upon exposure to bile salts, and survival rates across all treatments did not exceed 20%, indicating that bile salts exert toxic effects on strain AC31 and inhibit its normal growth.

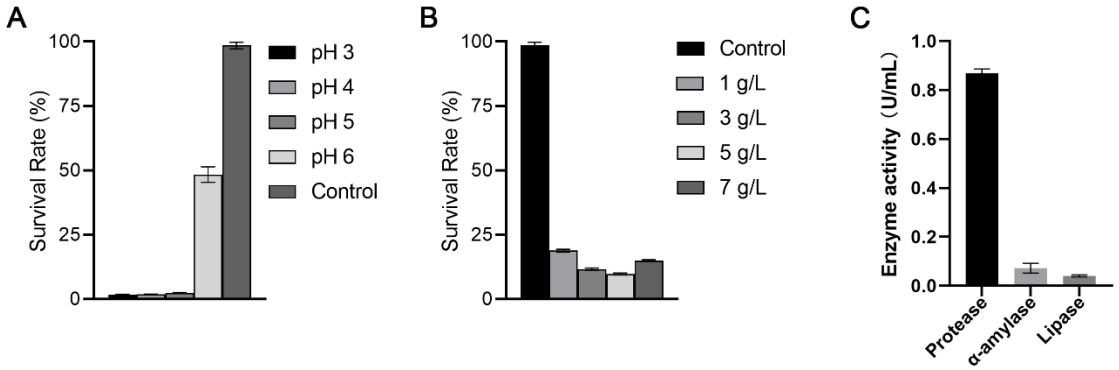


Fig. 9 Tolerance of strain AC31 to acid (A), bile salts (B) and protease, α-amylase, and lipase activities in the cell-free fermentation supernatant (C).

Next, the extracellular enzyme activities and antioxidant potential of strain AC31 were assessed.

Enzyme activity assays demonstrated that in the supernatants of AC31 liquid cultures at the log phase, the protease, α-amylase, and lipase activities were 0.87 ± 0.01 U/mL, 0.07 ± 0.01 U/mL, and 0.04 ± 0.01 U/mL, respectively (Fig. 9C). These findings thus confirm that strain AC31 synthesizes and secretes these digestive enzymes. In addition to its enzyme-producing capacity, the log-phase culture supernatant of AC31 exhibited measurable *in vitro* antioxidant activity, with a DPPH radical scavenging rate of 53.07 ± 2.99% (61 μM Trolox equivalents; Trolox equivalent antioxidant capacity, TEAC) and an ABTS radical scavenging rate of 78.56 ± 5.21% (102 μM Trolox equivalents; TEAC), further supporting its probiotic potential.

The colonization potential of strain AC31 in the intestinal tract of mariculture animals was evaluated via both *in vitro* and *in vivo* assays. Cell surface hydrophobicity of AC31 was determined using three solvents: xylene, chloroform, and ethyl acetate. The highest hydrophobicity value was obtained with xylene (48.50%), whereas much lower values were recorded for chloroform (3.85%) and ethyl acetate (3.52%) (Fig. 10B). This profile, high affinity for xylene alongside low affinities for chloroform and ethyl acetate, suggests a predominantly hydrophobic surface with limited electron-acceptor/donor characteristics[41], which may favor initial hydrophobic interactions with host epithelial surfaces[42].

The auto-aggregation capacity of AC31 was monitored over a 24-h incubation period. As shown in Fig. 10A, the auto-aggregation percentage increased in a time-dependent manner. The aggregation rate was low at the initial stage (9.08% at 2 h) but rose gradually to 33.50% at 4 h, 40.58% at 6 h, and 46.74% at 8 h. It continued to increase to 59.06% at 12 h and peaked at 71.67% at 24 h. According to the commonly used classification, this 24-h rate places AC31 in the high-aggregation category[43] The high auto-aggregation capacity of AC31 suggests a surface phenotype that may facilitate bacterial cell-cell interactions and initial adhesion, potentially contributing to its persistence in the intestinal environment[44]. Collectively, these results indicate that AC31 may possess favorable cell-surface interactions and colonization potential.

To validate these *in vitro* findings and to further determine whether the improved growth performance of *A. japonicus* and *R. philippinarum* following AC31 supplementation of the culture water is associated with intestinal colonization, the intestinal colonization of this strain in the two species was investigated. The specific primer pair *cyt* c_{550}-F and *cyt* c_{550}-R was used to detect AC31 in the intestines of *A. japonicus* and *R. philippinarum* after strain administration. As shown in Fig. 11, AC31 was detectable in the intestines of both species in the treatment groups (Lanes 5 and 7), whereas no bands or only faint bands were observed in the corresponding control groups (Lanes 4 and 6). It should be noted that strain AC31 was originally isolated from the intestines of *A. japonicus* and *R. philippinarum*, its presence in the control groups is therefore expected, although at a markedly lower abundance than in the treatment groups. These findings demonstrate that AC31 supplementation increases its intestinal abundance and facilitates its attachment to the intestinal mucosa, which may ultimately contribute to the improved growth performance of the experimental animals.

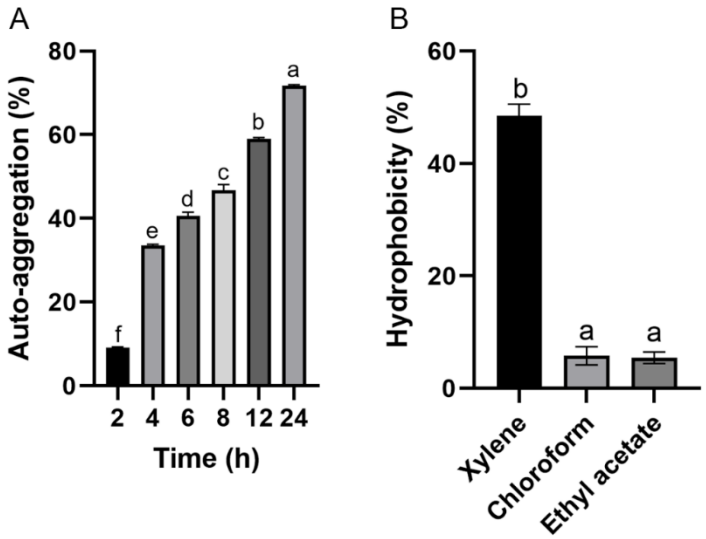


Fig. 10 Auto-aggregation (A) and hydrophobicity (B) ability of AC31

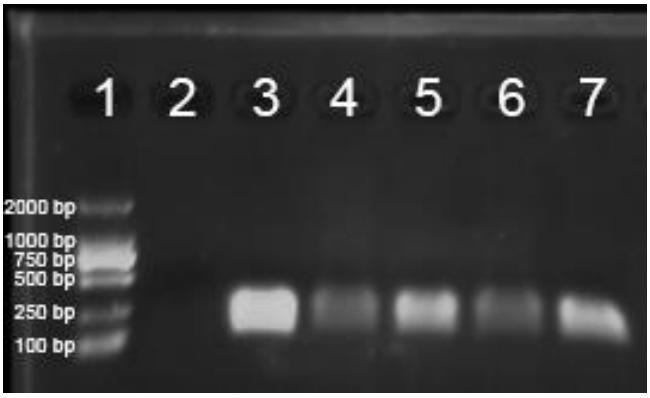


Fig. 11 Agarose gel electrophoresis of PCR products from different groups. Lane 1: 2,000 bp DNA marker; Lane 2: negative control using sterile ddH_2O as the template; Lane 3: positive control using total DNA of strain AC31 as the template; Lane 4: intestinal DNA from control *A. japonicus*; Lane 5: intestinal DNA from AC31-treated *A. japonicus*; Lane 6: intestinal DNA from control *R. philippinarum*; Lane 7: intestinal DNA from AC31-treated *R. philippinarum*.

Genomic insights into the probiotic potential of strain AC31

To further elucidate the molecular basis underlying the probiotic potential of strain AC31 observed in the above phenotypic assays, genomic analyses of this strain were performed. Gene Ontology (GO) annotation of the whole genome identified candidate genes associated with protein hydrolysis, starch utilization and lipid metabolism (Table S2). Multiple peptidase families and α-amylase-related proteins were annotated, alongside genes participating in glycerophospholipid metabolism, glycolipid metabolism and fatty acid degradation, supporting the metabolic capacity of AC31. Kyoto Encyclopedia of Genes and Genomes (KEGG) annotation further showed that AC31 harbors abundant metabolic pathways for amino acids, carbohydrates and lipids (Fig. 5D). Searching against the CAZy database uncovered 90 carbohydrate-active enzyme (CAZyme)-encoding genes, including 40 glycoside hydrolases (GHs), 28 glycosyltransferases (GTs), 15 carbohydrate esterases (CEs), four carbohydrate-binding modules (CBMs), two auxiliary activities (AAs), and one polysaccharide lyase (PL) (Fig. 12). These genes may endow strain AC31 with capabilities for carbohydrate hydrolysis, biosynthesis, modification and substrate binding.

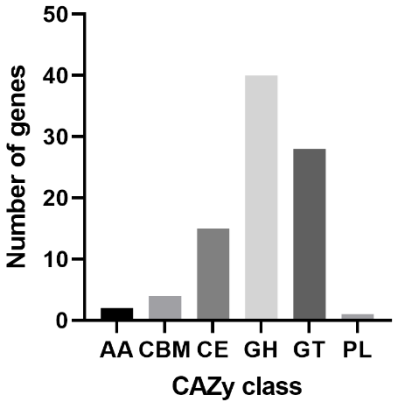


Fig. 12 Numbers of genes encoding carbohydrate-active enzymes (CAZymes) in the six CAZy categories: auxiliary activities (AA), carbohydrate-binding modules (CBM), carbohydrate esterases (CE), glycoside hydrolases (GH), glycosyltransferases (GT), and polysaccharide lyases (PL).

In addition to metabolic features, genomic determinants potentially associated with cell-surface interactions, intestinal persistence and redox homeostasis were examined. Genome annotation identified a sortase A gene (*srtA*), whose product is generally involved in anchoring LPXTG motif-containing proteins to the bacterial cell wall [45]; however, no canonical LPXTG motif-containing substrates were identified in the AC31 genome, and the contribution of the sortase system to surface interactions therefore remains unclear. Genes involved in flagellar biogenesis, assembly and motility were also identified, including *fliC*, *flgF*, *flgD*, *flhA*, *flhB*, *fliS* and *fliT*, as well as genes encoding motor and switch proteins (*motA*, *motB*, *fliG*, *fliM* and *fliN*), indicating that AC31 has the genetic potential for flagellar assembly and motility [46]. Beyond adhesion, KEGG-based genomic profiling uncovered genes involved in glutathione metabolism and redox systems, including genes encoding glutamate-cysteine ligase (gshA), 6-phosphogluconate dehydrogenase (gnd), glutathione peroxidase (gpx), thioredoxin (trxA), thioredoxin-disulfide reductase (trxB), and quinone oxidoreductases (qor and qorB) (Table 8). Collectively, the enzymatic assays and genomic annotations confirm the hydrolytic and metabolic potential of strain AC31, while the identified adhesion-associated genes and redox-related components further support its probiotic potential, consistent with the glutathione- and thioredoxin-based antioxidant systems encoded by its genome.

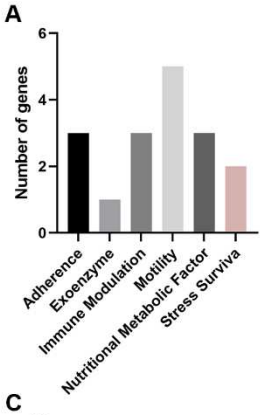
Table 8 Antioxidant related genes of AC31

Gene name	Locus tags	Annotation
spxA	AC31001233 AC31001556 AC31002141	Transcriptional regulator *spxA*
trxA	AC31002273	Thioredoxin
trxB	AC31000911	Thioredoxin reductase (NADPH)
qor	AC31000520	NAD(P)H dehydrogenase (quinone)
qorB	AC31000327	NADPH:quinone reductase
gpx	AC31002319	Glutathione peroxidase
gnd	AC31000560 AC31000574	6-phosphogluconate dehydrogenase
gshA	AC31000330	Glutamate-cysteine ligase

Genomic insights into the virulence factors and antibiotic resistance of strain AC31

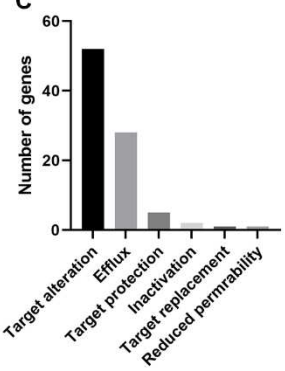
The safety of strain AC31 was preliminarily evaluated through genome-wide screening against the VFDB and CARD databases. VFDB annotation recovered a set of genes predominantly linked to environmental fitness and host interaction (Fig. 13A), including adhesion-associated genes such as *tufA*, *gapA* and *groEL*, alongside genes involved in motility and chemotaxis, namely *tlpA*, *tsr*, *cheM* and a response regulator. Genes for iron acquisition (e.g., siderophore and iron chelate transport systems) and stress survival factors (*clpC* and *clpP*) were also detected. Furthermore, several polysaccharide-related genes, including *rfbA* and *wecB*, were identified, which may facilitate surface adaptation and persistence within competitive niches (Fig. 13B). Importantly, no canonical exotoxins or other major classical virulence determinants were present in the AC31 genome.

CARD annotation revealed multiple antibiotic resistance genes in the AC31 genome (Fig. 13C), including *mphN, ErmB, cfrA, optrA*, multiple tetracycline efflux determinants, and several genes annotated as components of glycopeptide resistance gene clusters (Fig. 13D). These genomic findings are largely consistent with the phenotypic resistance to erythromycin, lincomycin and clindamycin, supported by the detection of *mphN*, *ermB* and *cfrA*. Although genes belonging to glycopeptide resistance clusters were detected, strain AC31 was phenotypically susceptible to vancomycin. This discrepancy implies that these loci may be incomplete, nonfunctional or transcriptionally silent under the tested conditions. In addition, *mphN* and *ermB* were localized on a plasmid. MOB-suite analysis categorized this replicon as mobilizable and assigned it to the MOBP relaxase family. Nevertheless, canonical conjugation genes, such as tra loci and type IV secretion system components, were absent, indicating that the plasmid is not self-transmissible. Even so, its mobilizable nature raises the possibility that plasmid-carried resistance genes could be transferred when compatible conjugative elements are provided in trans.



B

Category	Locus tags	Predicted function
Adherence	AC31000101	Elongation factor Tu;
	AC31000923	Type I glyceraldehyde 3 phosphate dehydrogenase;
	AC31002770	Chaperonin GroEL
Motility	AC31000474	
	AC31001207	Chemoreceptor;
	AC31000523	Methyl accepting chemotaxis protein;
	AC31001754	Response regulator
Stress survival	AC31001962	
	AC31000076	Clp ATP binding protein;
	AC31000919	Clp protease proteolytic subunit
Iron acquisition	AC31000713	
	AC31000714	Iron chelate uptake permease;
	AC31000715	Siderophore ABC transporter
Surface adaptation	AC31000593	*RfbA*;
	AC31000658	Polysaccharide biosynthesis protein;
	AC31000660	*WecB*
Exoenzyme	AC31000927	Phosphopyruvate hydratase



D

Gene	Drug class	Locus tags	Location
mphN	Macrolide	AC31003130	Plasmid
ErmB	Lincosamide, Macrolide	AC31003154	Plasmid
cfrA	Lincosamide, Oxazolidinone	AC31001430	Chromosome
		AC31002019	
		AC31000250	
optrA	Oxazolidinone, Phenicol	AC31002792	Chromosome
		AC31002914	
		AC31002958	
tet family	Tetracycline	AC31000747	Chromosome
		AC31001378	
		AC31001379	
		AC31002490	
		AC31002615	
vanR cluster hits	Glycopeptide	AC31001340	Chromosome
		AC31001611	
		AC31001685	
		AC31002496	
		AC31002874	
		AC31003108	

Fig. 13 Genomic insights into the virulence factors and antibiotic resistance of strain AC31. (A) Functional classification of genes annotated by VFDB in the AC31 genome. (B) Representative

virulence-associated genes involved in host interaction, environmental adaptation and stress survival identified by VFDB annotation. (C) Distribution of antibiotic resistance mechanisms predicted by CARD annotation in the AC31 genome. (D) Representative antibiotic resistance genes and their genomic locations in AC31.

Discussion

In this study, *Exiguobacterium* sp. AC31 was independently recovered from the intestinal tracts of two phylogenetically distant invertebrates, *A. japonicus* and *R. philippinarum*, and exhibited growth-promoting potential in both hosts. This distinguishes AC31 from many previously reported aquaculture probiotics, which are generally identified and validated within a single host species [47–49]. The independent recovery of the same strain from both hosts is particularly noteworthy, as it suggests that AC31 may possess a relatively strong capacity for environmental adaptation and compatibility with different host intestinal environments. AC31 therefore appears to represent not merely a conventional host-specific probiotic candidate, but rather a potential shared beneficial bacterium associated with distinct marine invertebrate hosts, making it a potentially important addition to the currently available probiotic resources for marine aquaculture.

The growth-promoting effect of *Exiguobacterium* sp. AC31 in both hosts may be related to its digestive enzyme-producing capacity. In aquatic animals, intestinal microorganisms can contribute to host nutrition by secreting extracellular enzymes that participate in the degradation of proteins, carbohydrates and lipids in ingested food particles [50, 51]. This function may be particularly important for marine deposit-feeding or filter-feeding animals, whose diets often contain structurally complex organic matter that is not readily utilized by the host alone [50, 52]. In the present study, AC31 exhibited extracellular protease, amylase and lipase activities, and corresponding enzyme activities were detected in the fermentation supernatant. Genome annotation additionally identified multiple genes related to carbohydrate, protein and lipid metabolism, further supporting its digestive potential. These phenotypic and genomic characteristics suggest that AC31 may enhance nutrient digestion and utilization in the host intestine, thereby contributing to the improved growth performance observed in both host species.

The beneficial effects of *Exiguobacterium* sp. AC31 may also be related to its ability to associate with the host intestinal environment. In aquaculture probiotics, surface-associated properties are often considered important for host interaction, intestinal persistence and competitive exclusion of undesirable microorganisms [53]. In the present study, AC31 exhibited surface characteristics consistent with this possibility, and genome annotation provided additional, although indirect, support. In particular, AC31 harbored several genes involved in flagellar assembly and motility, including *fliC*, which encodes flagellin, the major structural component of the flagellar filament; flagellin has been reported to facilitate initial surface attachment in some bacterial specie [54]. Additionally, elongation factor-encoding genes such as *tuf*, *fusA* and *tsf* were identified; although primarily involved in protein synthesis, these proteins have been reported to exhibit moonlighting functions related to adhesion in various bacteria [55]. PCR-based detection showed that the signal of AC31 in intestinal samples increased after supplementation, supporting intestinal association and short-term persistence of the strain in both hosts and thereby increasing the opportunity for direct interaction with the host and ingested nutrients. However, the available evidence does not yet justify a firm conclusion regarding stable long-term colonization. Moreover, because *A. japonicus* and *R. philippinarum* do not possess the highly acidic gastric environment typical of vertebrates [56],

conventional probiotic screening criteria such as tolerance to low pH and bile salts may not fully reflect intestinal adaptation potential in these marine invertebrates.

In addition to probiotic efficacy, biosafety is a critical requirement for practical application in aquaculture [57]. Previous studies have emphasized that candidate probiotics should be evaluated not only for beneficial effects, but also for pathogenicity, virulence-related determinants and the potential dissemination of antibiotic resistance genes [58]. *Exiguobacterium* sp. AC31 did not cause obvious acute mortality in immersion assays and did not induce apparent chronic toxicity during the 60-day culture trial, suggesting no obvious pathogenicity under the tested conditions. Genome-based safety evaluation further showed that no canonical exotoxins or other major classical virulence determinants were detected. Nevertheless, antibiotic resistance-related genes were identified in the AC31 genome, and some of these genes were located on a mobilizable plasmid. Similar safety concerns have been raised for other probiotic or probiotic-like bacteria, particularly members of the genus *Enterococcus* [59], in which beneficial properties have been discussed alongside the potential dissemination of mobile resistance determinants [60]. Therefore, although AC31 appeared non-pathogenic in the present host assays, its biosafety for practical application cannot yet be fully established, and the transferability of plasmid-borne resistance determinants should be experimentally assessed in future work.

Exiguobacterium sp. AC31 exhibits considerable probiotic potential; however, further evaluation is required before its practical application in aquaculture. Its beneficial effects have thus far been demonstrated only in *A. japonicus* and *R. philippinarum*. Validation in other economically important marine species and under commercial farming conditions is therefore needed to determine its host range, efficacy and consistency. Although the present findings support its intestinal persistence and digestive enzyme-producing capacity, the mechanisms underlying its growth-promoting effects remain unclear. Future studies should investigate its effects on nutrient utilization, host–microbiota interactions, immune regulation and metabolite production. The long-term biosafety and ecological impact of AC31 also warrant careful assessment, particularly regarding the stability and potential horizontal transfer of resistance-associated genes under aquaculture conditions. These findings expand the repertoire of host-associated probiotic candidates for marine aquaculture and provide a basis for investigating beneficial bacterial lineages shared among marine invertebrate hosts.

Conclusion

In conclusion, *Exiguobacterium* sp. AC31 was first isolated from the intestinal tract of *A. japonicus*, and a highly similar isolate, R27, was subsequently recovered from *R. philippinarum*. Molecular and genomic analyses indicated that the two isolates belonged to the same strain. AC31 exhibited multiple probiotic-associated traits, including extracellular digestive enzyme production, antioxidant activity, surface-associated properties and growth-promoting potential in both host species. Genome analysis further supported these phenotypic characteristics by revealing genes related to nutrient metabolism, environmental adaptation and other probiotic-associated functions. Although AC31 showed no obvious pathogenicity under the tested conditions, the presence of antibiotic resistance-related genes on a mobilizable plasmid indicates that further biosafety assessment is still required. Overall, this study helps to expand the repertoire of host-associated probiotic candidates for marine aquaculture and highlights AC31 as a potential cross-host beneficial bacterium.

Acknowledgments

This study was supported by the Liaoning Provincial Department of Education Fundamental Research Project of Universities (Dlou2610158013), the Liaoning Provincial Department of Education University Basic Scientific Research Project (2024JBZDZ001), the Liaoning Provincial Science and Technology Joint Program — Technology Tackling Project (2024JH2/102600078), the Central Government Subsidy Project for Liaoning Fisheries (2024, 2025), the Liaoning Provincial Major Science and Technology Special Project (Germplasm Innovation Program) (2024JH1/11700010), the Modern Agroindustry Technology Research System (CARS-49), and the 2022 Liaoning Applied Basic Research Program of Liaoning Provincial Department of Science and Technology (2022JH2/101300141).

References

1. Tigchelaar M, Cheung WWL, Mohammed EY, et al (2021) Compound climate risks threaten aquatic food system benefits. Nat Food 2:673–682. https://doi.org/10.1038/s43016-021-00368-9
2. FAO The State of World Fisheries and Aquaculture 2024. FAO
3. Basurto X, Gutierrez NL, Franz N, et al (2025) Illuminating the multidimensional contributions of small-scale fisheries. Nature 637:875–884. https://doi.org/10.1038/s41586-024-08448-z
4. Ren W, Xu Y, Weng S (2025) How does industrial intelligence affect the ecological efficiency of China's mariculture industry? Empirical analysis based on panel data from coastal regions of China. Marine Pollution Bulletin 212:117513. https://doi.org/10.1016/j.marpolbul.2024.117513
5. Bai Y, Du Y, Xiong Y, et al (2024) Integrated impacts of mariculture on nitrogen cycling processes in the coastal groundwater of Beihai, southern China. Science of The Total Environment 957:177622. https://doi.org/10.1016/j.scitotenv.2024.177622
6. Ren W, Xu Y (2024) Evaluation and optimization of mariculture ecological efficiency under technological heterogeneity — New evidence from China's coastal regions. Marine Pollution Bulletin 205:116563. https://doi.org/10.1016/j.marpolbul.2024.116563
7. Xie W, Jiang H (2021) Research Progress on the Application of Microecological Preparations in Aquaculture. Anhui Agricultural Science Bulletin 27:103–108. https://doi.org/10.16377/j.cnki.issn1007-7731.2021.22.037
8. Zhao H, Huo D, Cui W, et al (2025) Genome-wide association analysis provides genetic insights into variation of nutritional quality traits in sea cucumber *Apostichopus japonicus*. J Ocean Limnol. https://doi.org/10.1007/s00343-025-4274-2
9. Jiang K, Jiang L, Nie H, et al (2020) Molecular cloning and expression analysis of tyrosinases (tyr) in four shell-color strains of Manila clam *Ruditapes philippinarum*. PeerJ 8:e8641. https://doi.org/10.7717/peerj.8641
10. Li Y-X, Wang N-N, Zhou Y-X, et al (2021) *Planococcus maritimus* ML1206 Isolated from Wild Oysters Enhances the Survival of *Caenorhabditis elegans* against *Vibrio anguillarum*. Mar Drugs 19:150. https://doi.org/10.3390/md19030150
11. Yousuf S, Tyagi A, Singh R (2023) Probiotic Supplementation as an Emerging Alternative to Chemical Therapeutics in Finfish Aquaculture: a Review. Probiotics & Antimicro Prot 15:1151–1168. https://doi.org/10.1007/s12602-022-09971-z
12. Rahman MA, Ashrafudoulla M, Akter S, et al (2024) Probiotics and biofilm interaction in aquaculture for sustainable food security: A review and bibliometric analysis. Crit Rev Food Sci Nutr 64:12319–12335. https://doi.org/10.1080/10408398.2023.2249114
13. Cornet V, Khuyen TD, Mandiki SNM, et al (2021) GAS1: A New β-Glucan Immunostimulant Candidate to Increase Rainbow Trout (*Oncorhynchus mykiss*) Resistance to Bacterial Infections With Aeromonas salmonicida achromogenes. Front Immunol 12:693613. https://doi.org/10.3389/fimmu.2021.693613
14. Sumon TA, Hussain MdA, Sumon MdAA, et al (2022) Functionality and prophylactic role of probiotics in shellfish aquaculture. Aquaculture Reports 25:101220. https://doi.org/10.1016/j.aqrep.2022.101220
15. Wang N, Wu Y, Liu Y, et al (2026) Probiotic strain identification and safety assessment of unlabeled bacteria in infant products. International Journal of Food Microbiology 445:111500. https://doi.org/10.1016/j.ijfoodmicro.2025.111500

16. Lee S-J, Lee Y-S, Kim Y-R, et al (2025) Development of Novel Host-Associated Low-Temperature Probiotics (HALP) Tailored to Aquaculture Applications. Probiotics & Antimicro Prot. https://doi.org/10.1007/s12602-025-10828-4
17. Lemme-Dumit JM, Cazorla SI, Perdigón GDV, Maldonado-Galdeano C (2021) Probiotic Bacteria and Their Cell Walls Induce Th1-Type Immunity Against Salmonella Typhimurium Challenge. Front Immunol 12:660854. https://doi.org/10.3389/fimmu.2021.660854
18. Liu S, Xiong Y, Cao S, et al (2022) Dietary Stevia Residue Extract Supplementation Improves Antioxidant Capacity and Intestinal Microbial Composition of Weaned Piglets. Antioxidants (Basel) 11:2016. https://doi.org/10.3390/antiox11102016
19. Boucard A-S, Kulakauskas S, Alazzaz J, et al Isolation of derivatives from the food-grade probiotic *Lactobacillus johnsonii* CNCM I-4884 with enhanced anti-Giardia activity. Gut Microbes 17:2474149. https://doi.org/10.1080/19490976.2025.2474149
20. Castro-Severyn J, Pardo-Esté C, Araya-Durán I, et al (2022) Biochemical, genomic and structural characteristics of the Acr3 pump in *Exiguobacterium* strains isolated from arsenic-rich Salar de Huasco sediments. Front Microbiol 13:1047283. https://doi.org/10.3389/fmicb.2022.1047283
21. Salim S, Sugathan S (2025) Characterisation of *Exiguobacterium abrahamii* sp. nov., a novel strain isolated from mangrove soil with lanthipeptide biosynthetic genes. Antonie van Leeuwenhoek 118:76. https://doi.org/10.1007/s10482-025-02079-8
22. Shen L, Liu Y, Chen L, et al (2024) Genomic basis of environmental adaptation in the widespread poly-extremophilic Exiguobacterium group. ISME J 18:wrad020. https://doi.org/10.1093/ismejo/wrad020
23. Srivastava N, Shiburaj S, Khare SK (2024) Improved production of alkaline and solvent-stable proteases from a halotolerant *Exiguobacterium* isolate through heterologous expression. International Journal of Biological Macromolecules 260:129507. https://doi.org/10.1016/j.ijbiomac.2024.129507
24. Tedesco P, Palma Esposito F, Masino A, et al (2021) Isolation and Characterization of Strain *Exiguobacterium* sp. KRL4, a Producer of Bioactive Secondary Metabolites from a Tibetan Glacier. Microorganisms 9:890. https://doi.org/10.3390/microorganisms9050890
25. Li Y, Huang F, Jin Y, et al (2025) Characterization of Cold-Adapted Lipase from *Exiguobacterium* sp. and Its Cold Adaptation Mechanism. J Agric Food Chem 73:10369–10377. https://doi.org/10.1021/acs.jafc.4c11222
26. Sen SK, Jana A, Bandyopadhyay P, et al (2016) Thermostable amylase production from hot spring isolate *Exiguobacterium* sp: A promising agent for natural detergents. Sustainable Chemistry and Pharmacy 3:59–68. https://doi.org/10.1016/j.scp.2016.04.002
27. Anil Kumar PK, Suresh PV (2014) Biodegradation of Shrimp Biowaste by Marine *Exiguobacterium* sp. CFR26M and Concomitant Production of Extracellular Protease and Antioxidant Materials: Production and Process Optimization by Response Surface Methodology. Mar Biotechnol 16:202–218. https://doi.org/10.1007/s10126-013-9531-2
28. Hyson P, Shapiro JA, Wien MW (2015) Draft Genome Sequence of *Exiguobacterium* sp. Strain BMC-KP, an Environmental Isolate from Bryn Mawr, Pennsylvania. Genome Announc 3:e01164-15. https://doi.org/10.1128/genomeA.01164-15
29. Xie G, Zhang M, Zhong Z, et al (2024) Functional genomic characterization reveals the probiotic tendency and safety assessment of *Exiguobacterium acetylicum* G1–33 isolated from the

gut of the hybrid grouper (*Epinephelus fuscoguttatus*♀ × *E. lanceolatus*♂). Aquaculture Reports 36:102127. https://doi.org/10.1016/j.aqrep.2024.102127
30. Cheng A-C, Chaemlek P, Pichitkul P, Liu C-H (2026) Dietary incorporation of gut-derived probiotics from fast-growing white shrimp, *Penaeus vannamei* to boost growth and health performance in white shrimp. Fish & Shellfish Immunology 172:111214. https://doi.org/10.1016/j.fsi.2026.111214
31. Somalou P, Ieronymaki E, Feidaki K, et al (2024) Novel Wild-Type *Pediococcus* and *Lactiplantibacillus* Strains as Probiotic Candidates to Manage Obesity-Associated Insulin Resistance. Microorganisms 12:231. https://doi.org/10.3390/microorganisms12020231
32. Tenea GN, Gonzalez GL, Moreno JL (2022) Probiotic Characteristics and Antimicrobial Potential of a Native *Bacillus* subtilis Strain Fa17.2 Rescued from Wild *Bromelia* sp. Flowers. Microorganisms 10:860. https://doi.org/10.3390/microorganisms10050860
33. Li W, Wang J, Li C, et al (2022) Achieving Ultrasensitive Chromogenic Probes for Rapid, Direct Detection of Carbapenemase-Producing Bacteria in Sputum. JACS Au 3:227–238. https://doi.org/10.1021/jacsau.2c00607
34. He L, Jiang H, Li Y, et al (2024) Sulforaphane-Enriched Extracts from *Broccoli* Exhibit Antimicrobial Activity against Plant Pathogens, Promising a Natural Antimicrobial Agent for Crop Protection. Biomolecules 14:352. https://doi.org/10.3390/biom14030352
35. Pisu V, Dhanorkar A, Shetty D, et al (2025) Functional and Genomic Insights into *Clostridium butyricum* MCC0233: Probiotic Features and Safety Assessment. Probiotics & Antimicro Prot. https://doi.org/10.1007/s12602-025-10842-6
36. Zhang F, Yang H, Wang W, et al (2026) Whole-Genome Analysis and Probiotic Assessment of *Pediococcus acidilactici* PA_ZFRA1 Isolated from Bovine Rumen. Probiotics & Antimicro Prot 18:2220–2234. https://doi.org/10.1007/s12602-025-10673-5
37. Long X, Wu H, Zhou Y, et al (2022) Preventive Effect of *Limosilactobacillus* fermentum SCHY34 on Lead Acetate-Induced Neurological Damage in SD Rats. Front Nutr 9:852012. https://doi.org/10.3389/fnut.2022.852012
38. Kumari VBC, Huligere SS, Ramu R, et al (2022) Evaluation of Probiotic and Antidiabetic Attributes of *Lactobacillus* Strains Isolated From Fermented Beetroot. Front Microbiol 13:. https://doi.org/10.3389/fmicb.2022.911243
39. Li H, Qiao G, Gu J-Q, et al (2010) Phenotypic and genetic characterization of bacteria isolated from diseased cultured sea cucumber *Apostichopus japonicus* in northeastern China. Diseases of Aquatic Organisms 91:223–235. https://doi.org/10.3354/dao02254
40. Ennis NJ, Dharumadurai D, Sevigny JL, et al (2022) Draft Genomes Sequences of 11 *Geodermatophilaceae* Strains Isolated from Building Stones from New England and Indian Stone Ruins found at historic sites in Tamil Nadu, India. J Genomics 10:69–77. https://doi.org/10.7150/jgen.76121
41. Zuo F, Appaswamy A, Gebremariam HG, Jonsson A-B (2019) Role of Sortase A in Lactobacillus gasseri Kx110A1 Adhesion to Gastric Epithelial Cells and Competitive Exclusion of Helicobacter pylori. Front Microbiol 10:. https://doi.org/10.3389/fmicb.2019.02770
42. Deepika G, Karunakaran E, Hurley CR, et al (2012) Influence of fermentation conditions on the surface properties and adhesion of *Lactobacillus rhamnosus* GG. Microb Cell Fact 11:116. https://doi.org/10.1186/1475-2859-11-116
43. García-Cayuela T, Korany AM, Bustos I, et al (2014) Adhesion abilities of dairy *Lactobacillus*

plantarum strains showing an aggregation phenotype. Food Research International 57:44–50. https://doi.org/10.1016/j.foodres.2014.01.010
44. Davran Bulut S, Derebası BN, Günay S, et al (2026) Emerging Synbiotics Consisting of Catechin and Probiotic Bacteria: Exploring Aggregation, Adhesion, Antioxidant, and Anticancer Effects. Probiotics & Antimicro Prot 18:1797–1810. https://doi.org/10.1007/s12602-025-10631-1
45. Dandoy D, Fremaux C, Henry de Frahan M, et al (2011) The fast milk acidifying phenotype of Streptococcus thermophilus can be acquired by natural transformation of the genomic island encoding the cell-envelope proteinase PrtS. Microb Cell Fact 10:S21. https://doi.org/10.1186/1475-2859-10-S1-S21
46. Zhu S, Sun X, Li Y, et al The common origin and degenerative evolution of flagella in Actinobacteria. mBio 14:e02526-23. https://doi.org/10.1128/mbio.02526-23
47. Elsegeny SR, Radwan FS, Elshamy YM, et al (2025) A comprehensive overview of probiotics in aquaculture: from efficacy evaluation to diverse applications. Ann Microbiol 75:35. https://doi.org/10.1186/s13213-025-01825-7
48. Hoseinifar SH, Hoseini SM, Taheri Mirghaed A, et al (2024) Comparison of the effects of host-associated (autochthonous) and commercial probiotics on immune responses, growth parameters and intestinal microbiota of Caspian whitefish (*Rutilus frisii kutum*) fry. Front Mar Sci 11:. https://doi.org/10.3389/fmars.2024.1446927
49. Mahfuz MdA, Nobony TA, Jilani AK, et al (2025) Isolation and Validation of Host-Derived Probiotics From the Giant Freshwater Prawn (*Macrobrachium rosenbergii*): Impacts on Water Quality and Growth Performance. Aquac Nutr 2025:9156848. https://doi.org/10.1155/anu/9156848
50. Rai N, Kachore A, Julka JM, et al (2025) Symbiotic strategies: deciphering the role of gut microbiota in the nutrition and metabolism of fish and shellfish. Front Cell Infect Microbiol 15:. https://doi.org/10.3389/fcimb.2025.1639426
51. Zhang B-Y, Cai G-H, Yang H-L, et al (2024) New insights on intestinal microorganisms and carbohydrate metabolism in fish. Aquacult Int 32:2151–2170. https://doi.org/10.1007/s10499-023-01262-w
52. Qiao F, Liu Y k., Sun Y h., et al (2017) Influence of different dietary carbohydrate sources on the growth and intestinal microbiota of *Litopenaeus vannamei* at low salinity. Aquaculture Nutrition 23:444–452. https://doi.org/10.1111/anu.12412
53. Lebeer S, Vanderleyden J, De Keersmaecker SCJ (2010) Host interactions of probiotic bacterial surface molecules: comparison with commensals and pathogens. Nat Rev Microbiol 8:171–184. https://doi.org/10.1038/nrmicro2297
54. Deficiency of the flagellin subunit *FliC* exacerbates the pathogenicity of extraintestinal pathogenic *Escherichia coli* in BALB/c mice by inducing a more intense inflammation. International Journal of Biological Macromolecules 289:138761. https://doi.org/10.1016/j.ijbiomac.2024.138761
55. Morales M, Sentchilo V, Hadadi N, van der Meer JR (2021) Genome-wide gene expression changes of *Pseudomonas veronii* 1YdBTEX2 during bioaugmentation in polluted soils. Environ Microbiome 16:8. https://doi.org/10.1186/s40793-021-00378-x
56. Fu X, Xue C, Miao B, et al (2005) Characterization of proteases from the digestive tract of sea cucumber (*Stichopus japonicus*): High alkaline protease activity. Aquaculture 246:321–329. https://doi.org/10.1016/j.aquaculture.2005.01.012
57. Kesarcodi-Watson A, Kaspar H, Lategan MJ, Gibson L (2008) Probiotics in aquaculture: The

892 need, principles and mechanisms of action and screening processes. Aquaculture 274:1–14.
893 https://doi.org/10.1016/j.aquaculture.2007.11.019
894 58. Wei C, Luo K, Wang M, et al (2022) Evaluation of Potential Probiotic Properties of a Strain of
895 *Lactobacillus plantarum* for Shrimp Farming: From Beneficial Functions to Safety Assessment.
896 Front Microbiol 13:854131. https://doi.org/10.3389/fmicb.2022.854131
897 59. Hanchi H, Mottawea W, Sebei K, Hammami R (2018) The Genus Enterococcus: Between
898 Probiotic Potential and Safety Concerns—An Update. Front Microbiol 9:.
899 https://doi.org/10.3389/fmicb.2018.01791
900 60. Bednorz C, Guenther S, Oelgeschläger K, et al (2013) Feeding the Probiotic Enterococcus
901 faecium Strain NCIMB 10415 to Piglets Specifically Reduces the Number of Escherichia coli
902 Pathotypes That Adhere to the Gut Mucosa. Appl Environ Microbiol 79:7896–7904.
903 https://doi.org/10.1128/AEM.03138-13

Supplementary Files

This is a list of supplementary files associated with this preprint. Click to download.

- Fig.S1.tif
- Fig.S2.tif
- TableS1.docx
- TableS2.docx